

# BLOWUP FOR FLAT SLOW MANIFOLDS WITH APPLICATIONS TO REGULARIZATION OF PIECEWISE SMOOTH SYSTEMS USING TANH AND A MODEL OF AIRCRAFT GROUND DYNAMICS

K. U. KRISTIANSEN

Department of Applied Mathematics and Computer Science,  
Technical University of Denmark,  
2800 Kgs. Lyngby,  
DK

**ABSTRACT.** In this paper we demonstrate a method for extending the blowup method, in the formulation of Krupa and Szmolyan, to flat slow manifolds that lose hyperbolicity beyond any algebraic order. Although these manifolds have infinite co-dimension, they do appear naturally in certain settings. For example in (a) the regularization of piecewise smooth systems by tanh, (b) a model of aircraft landing dynamics, and finally (c) in a model of earthquake faulting. We demonstrate the approach on a simple model system and the examples (a) and (b).

## 1. INTRODUCTION

In this paper we focus on slow-fast systems on  $(x, y) \in \mathbb{R}^{n_s \times n_f}$  of the form

$$\begin{aligned} x' &= \varepsilon f(x, y, \varepsilon), \\ y' &= g(x, y, \varepsilon), \end{aligned} \tag{1.1}$$

where  $()' = \frac{d}{d\tau}$  denotes differentiation with respect to the fast time  $\tau$ . System (1.1) is called the fast system. Near points where  $g(x, y, \varepsilon) = \mathcal{O}(1)$  the variables  $x \in \mathbb{R}^{n_s}$  and  $y \in \mathbb{R}^{n_f}$  vary on separate time scales. The variable  $y$  is therefore called fast, while  $x$  is said to be slow. On the other hand, near points where  $g(x, y, \varepsilon) = \mathcal{O}(\varepsilon)$  then the variables both evolve on the slow time scale  $t = \varepsilon\tau$ . This is described by the slow system:

$$\begin{aligned} \dot{x} &= f(x, y, \varepsilon), \\ \varepsilon \dot{y} &= g(x, y, \varepsilon), \end{aligned} \tag{1.2}$$

with  $\dot{()} = \frac{d}{dt}$ . Setting  $\varepsilon = 0$  in (1.1) and (1.2) gives rise to two different limiting systems:  $(1.1)_{\varepsilon=0}$ :

$$\begin{aligned} x' &= 0, \\ y' &= g(x, y, 0), \end{aligned} \tag{1.3}$$

called the *layer problem*, and  $(1.2)_{\varepsilon=0}$ :

$$\begin{aligned} \dot{x} &= f(x, y, 0), \\ 0 &= g(x, y, 0), \end{aligned} \tag{1.4}$$

---

*Date:* December 3, 2024.



called the *reduced problem*. The set

$$C = \{(x, y) | g(x, y, 0) = 0\},$$

is called the critical manifold. Eq. (1.4) is only defined on the set  $C$ , while  $C$  is a set of critical points of (1.3). Subsets  $S \subset C$  where the linearization of (1.3) about  $(x, y) \in S$  only has as many eigenvalues with zero real part as there are slow variables  $n_s$  are called *normally hyperbolic*. Due to the special structure of (1.3) normally hyperbolicity is equivalent to all eigenvalues  $\lambda_i$ ,  $i = 1, \dots, n_f$ , of  $\partial_y g(x, y)$ ,  $(x, y) \in S$ , satisfying  $\text{Re } \lambda_i \neq 0$ . A normally hyperbolic subset  $S$  of  $C$  can, by the implicit function theorem applied to  $g(x, y) = 0$  with  $\partial_y g(x, y) \neq 0$ , be written as a graph

$$S : \quad y = h_0(x), \quad x \in U. \quad (1.5)$$

Fenichel's geometric singular perturbation theory [8, 9] establishes for  $\varepsilon \ll 1$  (a) the smooth perturbation of  $S$  in (1.5) with  $U$  compact to

$$S_\varepsilon : \quad y = h_0(x) + \mathcal{O}(\varepsilon),$$

for  $\varepsilon \ll 1$ , and (b) the existence and smoothness of stable and unstable manifolds of  $S_\varepsilon$ , tangent at  $(x, y) \in S$  for  $\varepsilon = 0$  to the associated linear spaces of the linearization of (1.3). As a consequence, the dynamics of (1.2), in a vicinity of a normally hyperbolic critical manifold  $S$ , is accurately described for  $\varepsilon \ll 1$  as a concatenation of orbits, respecting the direction of time, of the layer problem and the reduced problem. For an extended introduction to the subject of slow-fast theory, the reader is encouraged to consult the references [13, 14, 27].

Fenichel's theory does not apply near singular points where  $C$  is nonhyperbolic. To deal with such degeneracies, and extend the theory of geometric singular perturbations, the blowup method [4, 5, 6], in particular in the formulation of Krupa and Szmolyan [23, 24, 25], have proven extremely useful. The method *blows up* the singularity to a higher dimensional geometric object, such as a sphere or a cylinder. By appropriately choosing weights associated to the transformation, it is in most situations possible to divide the resulting vector-field by a power of a polar-like variable measuring the distance to the singularity. This gives rise to a new vector-field, only equivalent to the original one away from the singularity, for which hyperbolicity has been (partially) gained on the blowup of the singularity. Sometimes this approach of blowing up singularities has to be used successively, see e.g. [1, 16]. In this paper we study situations where the blowup approach does not apply directly.

In combination Fenichel's geometric singular perturbation theory and the blowup method have been very successful in describing global phenomena in slow-fast models. A frequent occurring phenomena in such models are relaxation oscillations, characterized by repeated switching of slow and fast motions. A prototypical system where these type of periodic orbits occur is the van Pol system [25, 27] but they also appear in many other models, in particular in those arising from neuroscience [12].

Recently more complicated examples of relaxation oscillations have been studied using these geometric methods. In [17], for example, the authors consider a model for the embryonic cell division cycle at the molecular level in eukaryotes. This model is an example of a slow-fast system not in the standard form (1.1): The slow-fast behaviour is in some sense hidden. Furthermore, the chemistry imposes



particular nonlinearities that give rise to special self-intersections of the set of critical points. Using the blowup method, the authors show that this in turn results in a novel type of relaxation oscillation in which segments of the periodic orbit glue close to the self-intersections of the critical set. In [15] another interesting oscillatory phenomenon is studied involving an unbounded critical manifold. Finally, the reference [16] provides a detailed description of relaxation oscillations occurring in a model describing glycolytic oscillations with two small singular parameters. The references [15] and [16] both apply blowup methods. These examples illustrate that each problem is unique; models have their own peculiar degeneracies, and a unifying framework is not possible. Yet the blowup method provides a foundation from which these systems can be dealt with rigorously. However, recently in [1], the authors consider a model from [7] describing earthquake faulting in which the blowup method in its original formulation fails. The system in [1] has a degenerate Hopf bifurcation within an everywhere attracting, but unbounded, critical manifold, from which a vertical family of periodic orbits emerges. The perturbation of these periodic orbits is complicated by the loss of compactness. Using Poincaré compactification, the critical manifold can be studied at infinity. However, the analysis is further complicated by the fact that the eigenvalue measuring the hyperbolicity decays exponentially at infinity. The blowup method requires the homogeneity of algebraic terms to leading order, and this approach does therefore not directly apply to this model. Applying the method presented in the present paper, the authors of [1] nevertheless managed to obtain a new geometric insight into the peculiar relaxation oscillations that occur in this model. In particular, a manifold was found, different from the critical manifold of the system, and not directly visible prior to blowup, which organizes the dynamics at infinity. The basic idea of the method in the present paper is to embed the system into a higher dimensional model by augmenting a new dynamic variable in such a way that the resulting system is algebraic to leading order at the degeneracy and therefore amenable to blowup.

Another example, where blowup does not directly apply, is a slow-fast system undergoing a dynamic Hopf bifurcation. Similar problems occur in Hamiltonian systems with fast oscillatory behaviour. Such systems are studied in [10, 19, 18] using separate techniques. However, in the case of dynamic Hopf, a promising direction is to combine blowup with the technique, popularized by Neishtadt in [29, 30], of complex time. See e.g. [11].

**1.1. Overview.** In section 2 we present the general problem and illustrate our approach by considering an extension of a set of models considered by Kuehn in [26]. We do not aim to provide a general geometric framework for our approach. This must be part of future research. Instead we will focus on successful applications of our approach. In particular, in section 3 we apply the method to study regularization of piecewise smooth (PWS) systems. PWS systems are of great significance in applications [3]; they occur in mechanics (friction, impact), in biology (genetic regulatory networks) and in variable structure systems in control engineering [35]. But these systems also pose many problems, both computationally and mathematically. A frequent approach is therefore to apply regularization. This has for example been done in the references [20, 21, 22], to deal with problems associated with lack of uniqueness in PWS systems, and in [32]. These references, however, exclude regularization functions such as  $\tanh$  due its special asymptotic properties.



We will in this paper demonstrate how the approach of this paper can be used to study the regularization by  $\tanh$ .

In section 4 we finally consider a model from [31] of aircraft ground dynamics. The model is a  $6D$  rigid body model but displays  $2D$  slow-fast phenomena such as a canard-like explosion of limit cycles. The authors of [31] do not investigate the origin of the slow-fast structure but present the following  $2D$  slow-fast model:

$$\begin{aligned}\dot{u} &= -\varepsilon(\alpha - v), \\ \dot{v} &= -u - (v - a)e^{vb}.\end{aligned}\tag{1.6}$$

see [31, Eqs. (7) and (8)], as a “minimal model” capturing the key features. Here  $(u, v)$  describes the planar velocity of the center of mass of the aircraft in body fixed coordinates. See [31, Figs. (3) and (4)]. The critical manifold of this system loses hyperbolicity beyond any algebraic order as  $v \rightarrow -\infty$ . We will apply the method of this paper to describe the special canard explosion occurring in this model.

## 2. A METHOD FOR FLAT SLOW MANIFOLDS

Kuehn in [26, Proposition 6.3] studies the following slow-fast system

$$\begin{aligned}\dot{u} &= \varepsilon\mu, \\ \dot{v} &= 1 - v^n u,\end{aligned}\tag{2.1}$$

with  $\varepsilon \ll 1$ ,  $\mu \neq 0$ ,  $(u, v) \in \mathbb{R}^2$ , and  $n \in \mathbb{N}$ . Here we focus on  $v \geq c > 0$  and  $n \geq 2$ . In comparison with [26] we have also replaced  $x, y, s$  by  $v, u$  and  $n$ , respectively. The set

$$S_a : \quad u = v^{-n}, \quad v \geq c > 0,$$

is an attracting critical manifold of (2.1). Indeed the linearization of (2.1) about  $S_a$  gives  $-nv^{n-1}u$  as a single nontrivial negative eigenvalue. By Fenichel’s theory, fixed compact subsets of  $S_a$  smoothly perturb into an attracting, locally invariant slow manifolds  $S_{a,\varepsilon}$ . The reference [26] investigates how far as  $v \rightarrow \infty$  the manifold  $S_{a,\varepsilon}$  can be extended as a perturbation of  $S_a$ . For this the author applies the change of coordinates  $(u, v) = (x, y^{-1})$  to compactify  $v \geq c$ . This gives

$$\begin{aligned}\dot{x} &= \varepsilon\mu y^n, \\ \dot{y} &= y^2(x - y^n),\end{aligned}\tag{2.2}$$

after a nonlinear transformation of time that corresponds to multiplication of the right hand side by  $y^n$ . This *desingularizes* the dynamics within  $y = 0$ . In the  $(x, y)$ -variables,  $S_a$  becomes

$$S_a : \quad x = y^n.$$

We continue to use the same symbol for  $S_a$  in the new  $(x, y)$ -variables. The manifold  $S_a$  is nonhyperbolic at  $y = 0$ . This is due to the alignment of  $S_a$  with the critical fibers in the original  $(x, y)$ -variables. The result [26, Proposition 6.3] then states that  $S_{a,\varepsilon}$  extends within  $x \geq 0, y \geq 0$  as a perturbation of  $S_a$  up until a neighborhood of  $(x, y) = 0$  that scales like

$$(x, y) = \left( \mathcal{O}(\varepsilon^{n/(n+1)}), \mathcal{O}(\varepsilon^{1/(n+1)}) \right),\tag{2.3}$$

with respect to  $\varepsilon \rightarrow 0$ .



**2.1. Blowup.** To prove (2.3) Kuehn in [26] applies the following blowup transformation

$$x = \bar{r}^n \bar{x}, \quad y = \bar{r} \bar{y}, \quad \varepsilon = \bar{r}^{n+1} \bar{\varepsilon}, \quad (\bar{r}, (\bar{x}, \bar{y}, \bar{\varepsilon})) \in \overline{\mathbb{R}}_+ \times S^2, \quad (2.4)$$

of  $(x, y, \varepsilon) = 0$ . Here

$$S^2 = \{(\bar{x}, \bar{y}, \bar{\varepsilon}) | \bar{x}^2 + \bar{y}^2 + \bar{\varepsilon}^2 = 1\}.$$

We introduce the blowup method by considering this example. Let  $B = \overline{\mathbb{R}}_+ \times S^2$  denote the *blowup space*. Then the blowup (2.4) can be viewed as a mapping:

$$\Phi : B \rightarrow \mathbb{R}^3,$$

blowing up the nonhyperbolic line

$$x = y = \varepsilon = 0,$$

to a sphere  $(\bar{x}, \bar{y}, \bar{\varepsilon}) \in S^2$  within  $\bar{r} = 0$ . The map  $\Phi$  transforms the vector-field  $X$  in (2.2) to a vector-field  $\bar{X} = \Phi^*(X)$  on  $B$  by pull-back. Here  $\bar{X}|_{\bar{r}=0} = 0$  but the exponents, or weights, of  $\bar{r}$  in the blowup (2.13),  $n$ ,  $1$  and  $n+1$ , respectively, have been chosen so that  $\bar{X}$  has a power of  $\bar{r}$ , here  $\bar{r}^{n+1}$ , as a common factor. The vector-field can therefore be *desingularized* through the division of  $\bar{r}^{n+1}$ . In particular,  $\hat{X} \equiv \bar{r}^{-(n+1)} \bar{X}$  is well-defined and non-trivial  $\hat{X}|_{\bar{r}=0} \neq 0$ . To describe the dynamics on the blowup space we could use spherical coordinates on  $S^2$ . But as demonstrated in [23] the dynamics across the blowup sphere varies significantly in general and it is therefore almost mandatory to use directional charts. For (2.4), the chart  $\bar{y} = 1$  for example can be used to describe the subset  $B \cap \{\bar{y} > 0\}$  of the blowup space. The corresponding coordinate change is obtained by setting  $\bar{y} = 1$  in (2.4):

$$x = r_1^n x_1, \quad y = r_1, \quad \varepsilon = r_1^{n+1} \varepsilon_1, \quad (2.5)$$

using a stereographic-like projection to parametrize  $S^2 \cap \{\bar{y} > 0\}$ . Here we use subscripts to distinguish the variables in (2.5) from those appearing in (2.4).

Different blowups and charts will appear during the manuscript. We will use the same notation and often identical symbols for each blowup. Although this can potentially lead to confusion we also believe that it stresses the standardization of the method, emphasizing the similarities of the arguments and the geometric constructions. Blowup variables are given a bar, such as  $(\bar{x}, \bar{y}, \bar{\varepsilon})$  in (2.4). Charts such as (2.5) will be denoted by  $\kappa_i$ , using subscripts to distinguish between the charts and the corresponding local coordinates. Similarly, we will use the (standard) convention that manifolds, sets and other dynamical objects in chart  $\kappa_i$  are given a subscript  $i$ . An object (set, manifold), say  $M_i$  obtained in chart  $\kappa_i$ , will in the blowup variables be denoted by  $\bar{M}$ . Finally, if  $M_i$  in chart  $\kappa_i$  is visible in chart  $\kappa_j$  then it will be denoted by  $M_j$  in terms of the coordinates in this chart.

**2.2. A flat slow manifold.** Now, we return to (2.2) and ask the following question: What happens if we replace  $y^n$  in (2.2) by  $e^{-y^{-1}}$ ?

$$\dot{x} = \varepsilon \mu e^{-y^{-1}}, \quad (2.6)$$

$$\dot{y} = y^2(x - e^{-y^{-1}}).$$

The set

$$S_a : \quad x = e^{-y^{-1}}, \quad (2.7)$$



re-defining  $S_a$  again, is a critical manifold of (2.6). It is *flat* as a graph over  $y$  at  $y = 0$  in the sense that all derivatives of the right hand side of (2.7) vanish at  $y = 0$ . The linearization of (2.6) about  $S_a$  in (2.7) gives

$$-e^{-y^{-1}}, \quad (2.8)$$

as a single nontrivial eigenvalue. Hence  $S_a$  is therefore attracting for  $y > 0$  but loses hyperbolicity at an exponential rate as  $y \rightarrow 0^+$ . Then, as outlined in the introduction, the blowup method does not directly apply. The blowup method requires homogeneity of the leading order term to enable the desingularization, and letting  $n \rightarrow \infty$  in (2.2) and (2.3) is clearly hopeless. We will demonstrate our approach by extending the slow manifold of (2.6) near  $y = 0$ . Generalizations of the approach to more general examples of flat functions, such as  $y^\alpha e^{-y^{-\beta}}$  with  $\beta > 0$ , are straightforward.

The basic idea of our approach is to augment the exponential:

$$q = e^{-y^{-1}}, \quad (2.9)$$

which is also the negative of the eigenvalue (2.8), as a new dynamic variable. Differentiating (2.9) gives

$$\dot{q} = e^{-y^{-1}} y^{-2} \dot{y} = e^{-y^{-1}} (x - e^{-y^{-1}}) = q(x - q),$$

using (2.6) in the second equality and (2.9) in the third. But then using (2.9) in (2.6) we obtain an extended system

$$\begin{aligned} \dot{x} &= \varepsilon \mu q, \\ \dot{y} &= y^2(x - q), \\ \dot{q} &= q(x - q), \\ \dot{\varepsilon} &= 0, \end{aligned} \quad (2.10)$$

on  $(x, y, q, \varepsilon) \in \mathbb{R} \times \overline{\mathbb{R}}_+^3$ . Introducing  $q$  by (2.9) automatically embeds a hyperbolic-center structure into the system: To illustrate this simple fact, suppose time is so that  $y$  has algebraic, center-like decay as  $\mathcal{O}(1/t)$  for  $t \rightarrow \infty$ . Then  $q$  decays hyperbolically as  $\mathcal{O}(e^{-t})$ . This construction will therefore enable the use of center manifold theory and normal form methods to study systems like (2.6).

The set

$$Q : \quad q = e^{-y^{-1}}, \quad (2.11)$$

is by construction an invariant set of (2.10). However, the invariance of  $Q$  is implicit in (2.10) and we can invoke it when needed. Now  $S_a$  in (2.7) becomes

$$S_a : \quad x = q, \varepsilon = 0, \quad (2.12)$$

using the same symbol in the new variables  $(x, y, q, \varepsilon)$ . This is a critical manifold of the extended system (2.10). The linearization now has  $-q$  as a single nontrivial eigenvalue. The manifold  $S_a$  in (2.12) is nonhyperbolic at  $q = 0$  but now, again by construction, the loss of hyperbolicity is algebraic. We therefore apply the following blowup transformation:

$$y = \bar{y}, \quad x = \bar{r}\bar{x}, \quad q = \bar{r}\bar{q}, \quad \varepsilon = \bar{r}\bar{\varepsilon}, \quad (\bar{y}, \bar{r}, (\bar{x}, \bar{q}, \bar{\varepsilon})) \in \overline{\mathbb{R}}_+^2 \times S^2, \quad (2.13)$$

of  $(x, q, \varepsilon) = 0$ . In this case the blowup transformation blows up the line  $y \geq 0, x = q = \varepsilon = 0$  to a cylinder  $(\bar{y}, (\bar{x}, \bar{q}, \bar{\varepsilon})) \in \overline{\mathbb{R}}_+ \times S^2$  and desingularization is obtained



through division of the resulting vector-field by  $\bar{r}$ . In this section, we shall only focus on the following chart

$$\kappa_1 : \quad \bar{q} = 1 : \quad u = r_1 x_1, \quad q = r_1, \quad \varepsilon = r_1 \epsilon_1, \quad (2.14)$$

with  $r_1 \geq 0$ , to cover  $S^2 \cap \{\bar{q} > 0\}$  of the blowup sphere. Notice that  $y$  is not transformed and we will therefore for simplicity continue to use this symbol in chart  $\kappa_1$ .

**2.3. Chart  $\kappa_1$ .** Insertion of (2.14) into (2.10) gives

$$\begin{aligned} \dot{r}_1 &= r_1(x_1 - 1), \\ \dot{x}_1 &= (1 - x_1)x_1 + \epsilon_1 \mu, \\ \dot{y} &= y^2(x_1 - 1), \\ \dot{\epsilon}_1 &= (1 - x_1)\epsilon_1, \end{aligned} \quad (2.15)$$

after division of the right hand side by  $r_1$ . The set  $Q$  in (2.11) becomes

$$Q_1 : \quad r_1 = e^{-y^{-1}}.$$

**Remark 2.1.** Notice that in (2.15) the  $r_1$ -equation decouples. This is possible in the chart  $\bar{q} = 1$  in all the models and settings that I have considered. Indeed, beyond the leading order, one can just eliminate  $r_1$  using the invariance of  $Q_1$ . For system (2.10), this effectually means that the dimension of the resulting system is the same as the dimension of the chart  $\bar{y} = 1$  associated with the blowup in (2.4) of (2.1).

Note that  $v = \delta$  corresponds to

$$r_1 = e^{-\delta^{-1}},$$

within  $Q_1$ . Let

$$\rho(\delta) = e^{-\delta^{-1}}.$$

Then we consider the following set

$$U_1 = \{(r_1, x_1, v, \epsilon_1) | r_1 \in [0, \rho(\delta)], \epsilon_1 \in [0, \nu], v \in [0, \delta], x_1 \in [0, \xi^{-1}]\},$$

with  $\delta, \nu$  and  $\xi$  all sufficiently small.

The critical manifold  $S_a$  in (2.12) becomes

$$S_{a,1} : \quad x_1 = 1.$$

The advantage of the blowup is that we have gained hyperbolicity of  $S_{a,1}$  at  $r_1 = \epsilon_1 = 0$ . Indeed, the linearization of (2.15) about a point with  $x_1 = 1, r_1 = 0, \epsilon_1 = 0$  gives  $-1$  as a single non-zero eigenvalue. The associated eigenvector is in the  $x_1$ -direction. By center manifold theory we therefore directly obtain the following:

**Proposition 2.2.** *Within  $U_1$  there exists a center manifold*

$$M_1 : \quad x_1 = 1 - \epsilon_1 \mu(1 + \mathcal{O}(\epsilon_1)).$$

*$M_1$  has invariant foliations by  $Q_1$  and*

$$E_1 : \quad \varepsilon = r_1 \epsilon_1,$$

*due to the conservation of  $\varepsilon$ . Furthermore,  $M_1$  contains  $S_{a,1}$  within  $\epsilon_1 = 0$  as set of equilibria and*

$$C_1 : \quad x_1 = 1 - \epsilon_1 \mu(1 + \mathcal{O}(\epsilon_1)), \quad r_1 = v = 0, \quad (2.16)$$



as a center sub-manifold.  $C_1$  is overflowing (inflowing) if  $\mu > 0$  ( $\mu < 0$ ).

This result can be viewed as an extension of [26, Lemma 5.4] to a flat slow manifold. In the following we present some conclusions from this result.

**2.4. Conclusion.** The center manifold  $M_1$  is foliated by two invariant sets  $Q_1$  and  $E_1$ . The intersection  $M_1 \cap Q_1 \cap E_1$  is the extension of Fenichel's slow manifold, being  $\mathcal{O}(e^{-c/\varepsilon})$ -close to  $S_{a,\varepsilon}$  at  $r_1 = \rho(\delta)$ . It intersects  $\epsilon_1 = \nu$  with

$$x_1 = 1 - \nu\mu(1 + \mathcal{O}(\nu)), \quad e^{-v^{-1}} = \varepsilon\nu^{-1},$$

using the conservation of  $Q_1$  and  $E_1$ . Blowing back down using (2.14) we realize that we have extended the slow manifold as a center manifold up to

$$u = \varepsilon\nu^{-1}(1 - \nu\mu(1 + \mathcal{O}(\nu))), \quad v = \ln^{-1}(\varepsilon^{-1}\nu),$$

where it is  $\ln^{-1}(\varepsilon^{-1}\nu)$ -close to  $C_1$  in (2.16).

To continue  $C_1$  across the blowup sphere one may consider the “scaling” chart

$$\kappa_2 : \quad \varepsilon = 1.$$

For system (2.10) this chart corresponds to

$$y = y, \quad x = r_2 x_2, \quad q = r_2 q_2, \quad \varepsilon = r_2.$$

We will skip the details here for this introductory system and instead focus on our two main examples: Regularization of PWS systems by tanh and a model of aircraft ground dynamics, to be considered in the following sections. However, we will here note that  $\epsilon_1 = \nu$  in chart  $\bar{q} = 1$  in general, due to the conservation of  $\varepsilon$ , corresponds to  $r_1 = o(1)$  with respect to  $\varepsilon$ . In (2.10) we have  $r_1 = \varepsilon/\nu$  at  $\varepsilon = \nu$ . Therefore by the invariance of  $Q$ , we always have  $y = o(1)$  (typically logarithmically with respect to  $\varepsilon$ ) in  $\kappa_2$  and this will effectively enable the decoupling of  $y$  in scaling chart.

### 3. REGULARIZATION OF PWS SYSTEMS BY tanh

In this section we shall consider the following planar  $(x, y)$  PWS vector-field  $X = (X^+, X^-)$  with  $X^+ = (1, 2x)$  defined on  $\Sigma^+ : y > 0$ :

$$\begin{aligned} \dot{x} &= 1, \\ \dot{y} &= 2x, \end{aligned} \tag{3.1}$$

and  $X^- = (0, 1)$  defined on  $\Sigma^- : y < 0$ :

$$\begin{aligned} \dot{x} &= 0, \\ \dot{y} &= 1. \end{aligned} \tag{3.2}$$

This system is a PWS normal form for the planar *visible fold*. The discontinuity set

$$\Sigma : \quad y = 0,$$

is called the switching manifold and  $T = (0, 0) \in \Sigma$  is a *visible fold point* since the orbit  $y = x^2$  of  $X^+$  has quadratic tangency with  $\Sigma$  at  $T$  while  $X^-(T) \neq 0$ . The point  $T \in \Sigma$  divides  $\Sigma$  into a (stable) sliding region

$$\Sigma_{sl} : \quad x < 0,$$

and a crossing region

$$\Sigma_{cr} : \quad x > 0.$$



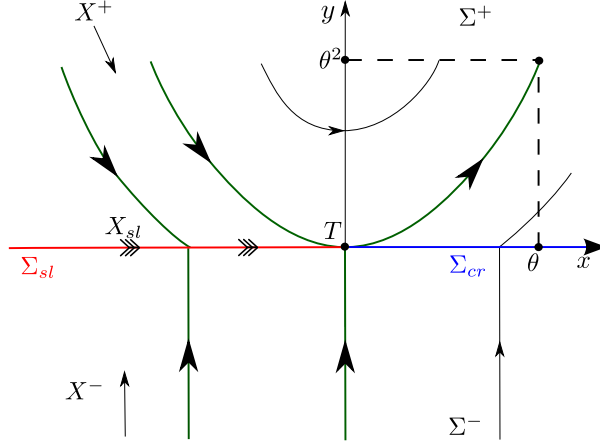


FIGURE 1. PWS phase portrait of (3.2) and (3.1).

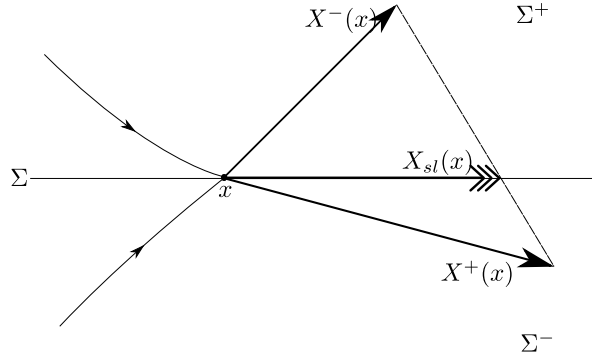


FIGURE 2. Illustration of the Filippov vector-field (3.3).

See Fig. 1. For  $p \in \Sigma_{sl}$  the vectors  $X^\pm(p)$  are in opposition and to continue orbits forward in time one has to define a vector-field  $X_{sl}$  on  $\Sigma_{sl}$ . A natural choice is to follow the Filippov convention and define the sliding vector-field:

$$X_{sl} = \lambda X^+ + (1 - \lambda) X^-, \quad \lambda(x) = \frac{X_2^-(x, 0)}{X_2^-(x, 0) - X_2^+(x, 0)}, \quad (3.3)$$

which has a nice geometric interpretation illustrated in Fig. 2. For (3.1) and (3.2) we have  $\lambda = \frac{1}{1-2x}$  and

$$X_{sl}: \quad \dot{x} = \frac{1}{1-2x}, \quad \dot{y} = 0, \quad (x, y) \in \Sigma_{sl}. \quad (3.4)$$

This gives the phase portrait illustrated in Fig. 1. Notice in particular that all orbits that reach  $\Sigma_{sl}$  leave  $\Sigma$  at  $T$  following  $X_{sl}$  and  $\{y = x^2 | x > 0\}$ .



**3.1. Regularization: Slow-fast analysis.** In [32] the authors regularize the PWS system  $X = (X^+, X^-)$ , described by (3.1) and (3.2), through a Sotomayor and Teixeira regularization:

$$X_\varepsilon = \frac{1}{2}X^+(1 + \phi(y\varepsilon^{-1})) + \frac{1}{2}X^-(1 - \phi(y\varepsilon^{-1})).$$

See [34]. Here  $\phi$  belongs to the following set  $C_{ST}^k$  of functions:

**Definition 3.1.** *The set  $C_{ST}^k$  of Sotomayor and Teixeira regularization functions  $\phi$  satisfy:*

1° Finite deformation:

$$\phi(y) = \begin{cases} 1 & \text{for } y \geq 1, \\ \in (-1, 1) & \text{for } y \in (-1, 1), \\ -1 & \text{for } y \leq -1, \end{cases} \quad (3.5)$$

2° Monotonicity:

$$\phi'(y) > 0 \quad \text{within } y \in (-1, 1). \quad (3.6)$$

3° Finite  $C^k$ -smoothness:  $\phi \in C^\infty$  within  $y \in (-1, 1)$  but there exists a smallest  $k \geq 1$  so that  $\phi^{(k+1)}$  is discontinuous at  $y = \pm 1$ :  $\phi^{(k+1)}(\pm 1^\mp) \neq 0$ .

An example of a  $C_{ST}^1$  regularization function within this class is the following function

$$\phi(y) = -\frac{1}{2}y^3 + \frac{3}{2}y \quad \text{for } y \in (-1, 1), \quad (3.7)$$

with  $\phi(y) = \pm 1$  for  $y \gtrless \pm 1$ . Here  $\phi^{(1)}(\pm 1^\mp) = 0$  but  $\phi^{(2)}(\pm 1^\mp) = \mp 3$  (while  $\phi^{(2)}(\pm 1^\pm) = 0$ ) and hence  $k = 1$  in 3° of Definition 3.1 for this example. Note, however, that 1° excludes analytic functions such as  $\tanh$ .

In terms of  $(x, \hat{y})$  where

$$\hat{y} = y\varepsilon^{-1}, \quad (3.8)$$

the system  $X_\varepsilon$  is slow-fast, with  $x$  slow and  $\hat{y}$  fast. For Eqs. (3.1) and (3.2) we have

$$\begin{aligned} \dot{x} &= \frac{1}{2}(1 + \phi(\hat{y})), \\ \varepsilon \dot{\hat{y}} &= x(1 + \phi(\hat{y})) + \frac{1}{2}(1 - \phi(\hat{y})), \end{aligned} \quad (3.9)$$

or in terms of the fast time  $\tau = \varepsilon^{-1}t$ :

$$\begin{aligned} x' &= \frac{\varepsilon}{2}(1 + \phi(\hat{y})), \\ \hat{y}' &= x(1 + \phi(\hat{y})) + \frac{1}{2}(1 - \phi(\hat{y})). \end{aligned} \quad (3.10)$$

Hence the layer problem for this model is

$$\begin{aligned} x' &= 0, \\ \hat{y}' &= x(1 + \phi(\hat{y})) + \frac{1}{2}(1 - \phi(\hat{y})), \end{aligned} \quad (3.11)$$



while

$$\begin{aligned}\dot{x} &= \frac{1}{2}(1 + \phi(\hat{y})), \\ 0 &= x(1 + \phi(\hat{y})) + \frac{1}{2}(1 - \phi(\hat{y})),\end{aligned}\tag{3.12}$$

is the reduced problem.

The Filippov convention appears naturally in mechanics, but it also has the following desirable property:

**Theorem 3.2.** [20, 28] *The regularized system  $X_\varepsilon$  possesses an attracting critical manifold  $S_a$  for  $\varepsilon = 0$  which is a graph over  $\Sigma_{sl}$ . The reduced equations for the slow variable  $x$  coincides with Filippov's sliding equations. The critical manifold is non-hyperbolic at  $x = 0$ .*

*Proof.* We demonstrate this result by considering our model system (3.9). The critical manifold:

$$\phi(\hat{y}) = \frac{1 + 2x}{1 - 2x},\tag{3.13}$$

is only a graph over  $\bar{\Sigma}_{sl}$ ; within  $\Sigma_{cr}$  the expression on the right hand side becomes  $\geq \pm 1$ . By linearizing (3.11) about (3.13) we realise that the manifold (3.13) is attracting within  $\Sigma_{sl}$  but nonhyperbolic at  $x = 0$  since  $\phi'(1) = 0$  there.

The reduced equations for the slow variable then becomes

$$\dot{x} = \frac{1}{2}(1 + \phi(\hat{y})) = \frac{1}{1 - 2x},\tag{3.14}$$

using (3.13). This expression coincides with (3.4).  $\square$

The proof does not use 1° and 3° of Definition 3.1 and this result therefore applies to a larger set of functions  $\phi$ , including analytic functions such as  $\tanh$ , satisfying:

$$\phi(\hat{y}) \in [-1, 1], \quad \phi'(\hat{y}) > 0 \text{ for } \hat{y} \in (-1, 1), \quad \phi(\hat{y}) \rightarrow \pm 1 \text{ for } \hat{y} \rightarrow \pm\infty.\tag{3.15}$$

By Fenichel's theory, compact subsets of  $S_a$  perturb to slow invariant manifolds  $S_{a,\varepsilon}$  for  $\varepsilon$  sufficiently small. The flow on  $S_{a,\varepsilon}$  converges to the flow of the reduced problem for  $\varepsilon \rightarrow 0$ . The authors in [32] investigate, among other things, the intersection of  $S_{a,\varepsilon}$  with a fixed section  $y = \theta$  for  $\phi \in C_{ST}^k$ ,  $0 \leq k < \infty$ . We find it easier to study the intersection of  $S_{a,\varepsilon}$  with  $x = \theta$  rather than  $y = \theta$ , but essentially the result of [32, Theorem 2.2] is the following:

**Theorem 3.3.** *Consider  $\phi \in C_{ST}^{n-1}$ ,  $n \geq 2$ . Let*

$$r_2 = \varepsilon^{1/(2n-1)}.$$

*Then the slow manifold  $S_{a,\varepsilon}$  intersects  $x = \theta$  in  $(\theta, y_\theta(\varepsilon))$  with*

$$y_\theta(\varepsilon) = \theta^2 + \varepsilon - r_2^n \left( \frac{2}{\phi^{[n]}} \right)^{2/(2n-1)} \eta(n)^2 (1 + r_2 F(r_2)),\tag{3.16}$$

where

- $F$  is smooth;
- $\phi^{[n]} = \frac{(-1)^{n+1}}{n!} \phi^{(n)}(1) > 0$ ;
- $\eta(n) > 0$  is a positive constant depending only on  $n$ .



*Proof.* This result is to order  $\varepsilon$  obtained by setting  $x_0^+ = \sqrt{y}$ ,  $\alpha^+ = -1/\sqrt{y}$ , in the expression for  $P_\varepsilon(x)$  in the second point of the itemize in [32, Theorem 2.2], and solving  $P_\varepsilon(x) = \theta$  for  $y$ .  $\square$

The authors in [32] use asymptotic methods. We will in Appendix A demonstrate an alternative proof using the blowup method which will give rise to the complete expression in (3.16).

**3.2. Geometry of regularization.** In this paper we investigate the intersection of  $S_{a,\varepsilon}$  with  $x = \theta$  for the analytic regularization function

$$\phi(\hat{y}) = \tanh(\hat{y}).$$

In terms of the application of slow-fast theory, this adds a significant amount of complexity since here  $\phi' > 0$  for all  $\hat{y} \in \mathbb{R}$ . This implies, in contrast to the case of  $C_{ST}^k$ -functions, that the critical manifold loses hyperbolicity at infinity  $\hat{y} \rightarrow \infty$ . For this it is useful to consider the scaling  $y = \varepsilon \hat{y}$  in (3.8) as part of a blowup:

$$y = \pi \bar{y}, \quad \varepsilon = \pi \bar{\varepsilon}, \quad \pi \geq 0, \quad (\bar{y}, \bar{\varepsilon}) \in S^1$$

Then  $y = \varepsilon \hat{y}$  becomes a chart

$$\bar{\varepsilon} = 1 : \quad y = \hat{\pi} \hat{y}, \quad \varepsilon = \hat{\pi}.$$

In the  $(x, \hat{y})$ -system the layer problem has  $\dot{x} = 0$  for  $\varepsilon = 0$ . The PWS is therefore not visible in this chart for  $\varepsilon = 0$ . To connect to the PWS system, one can consider the two charts

$$\bar{y} = \pm 1 : \quad y = \pm \hat{\pi}, \quad \varepsilon = \hat{\pi} \hat{\varepsilon}.$$

to cover  $\bar{y} > 0$  and  $\bar{y} < 0$ , respectively, of the sphere  $(\bar{y}, \bar{\varepsilon}) \in S^1$ . The advantage of the  $C_{ST}^k$ -functions is that the charts  $\bar{y} = \pm 1$  are not needed. Indeed, if  $\phi \in C_{ST}^k$  then  $\phi(\hat{y}) = \pm 1$  for  $\hat{y} \gtrless \pm 1$  cf. 1° in Definition 3.1, whence

$$X_\varepsilon = X^\pm \quad \text{for} \quad y \gtrless \pm \varepsilon.$$

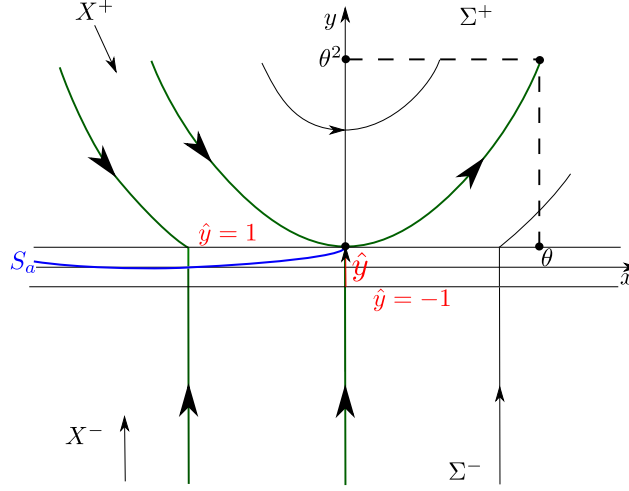
Therefore we can just *scale back down* and return to  $y$  (as it was done in [21]) whenever  $\hat{y} \notin (-1, 1)$  (corresponding to  $y \notin (-\varepsilon, \varepsilon)$  using (3.8)). This then leads to the following interpretation of phase space in the case of  $C_{ST}^k$ -functions: We continue orbits of  $X^\pm$  that reach  $y = \pm \varepsilon$ , respectively, within  $\hat{y} \in (-1, 1)$  using (3.10). Once an orbit of (3.10) reaches  $\hat{y} = \pm 1$  again then this orbit can be continued using the PWS vector-fields  $X^\pm$  from  $y = \pm \varepsilon$ , respectively. This also leads to a (singular) description for  $\varepsilon = 0$ . Geometrically, it corresponds to blowing up the plane  $y = 0$  to  $\hat{y} \in [-1, 1]$  for  $\varepsilon = 0$ . See Fig. 3. However, for regularization functions such as  $\tanh$  within the class (3.15), this construction is not possible and we need the charts to connect  $y = \mathcal{O}(\varepsilon)$  with  $y = \mathcal{O}(1)$ . But furthermore, which is relevant for our purposes in this paper,  $\tanh(\hat{y})$  is *flat* for  $\hat{y} \rightarrow \pm\infty$ . Indeed, let  $\hat{y} = \hat{\varepsilon}^{-1}$ . Then

$$\tanh(\hat{\varepsilon}^{-1}) = 1 - \frac{2e^{-2\hat{\varepsilon}^{-1}}}{1 + e^{-2\hat{\varepsilon}^{-1}}}, \quad (3.17)$$

with all derivatives at  $\hat{\varepsilon} = 0$  vanishing.

On the other hand, the system (3.9) with  $\phi(\hat{y}) = \tanh(\hat{y})$  is in fact so simple that it can be integrated directly (see Appendix B). This example therefore provides a useful forum in which to introduce our geometric approach. Needless to say, our method, relying only on hyperbolic methods and normal form theory, applies to regularization by  $\tanh$  of my complicated systems, such as nonlinear versions of  $X^\pm$  and systems in higher dimensions.



FIGURE 3. Singular slow-fast geometry for  $\phi \in C_{ST}^k$ .

**3.3. Main result.** Using the geometric methods developed in this paper we prove the following:

**Theorem 3.4.** *Consider the analytic regularization function  $\phi(\hat{y}) = \tanh(\hat{y})$ . Then the slow manifold of (3.9) intersects  $x = \theta$  in  $(\theta, y_\theta(\varepsilon))$  with*

$$y_\theta(\varepsilon) = \theta^2 + \varepsilon \left( \frac{1}{4} \ln \left( \frac{\pi}{2} \varepsilon^{-1} \right) + R(\sqrt{\varepsilon}) \right),$$

for some smooth function  $R(\sqrt{\varepsilon}) = \mathcal{O}(e^{-c\varepsilon^{-1}})$ .

We prove Theorem 3.4 using our geometric approach in the following. First we present the results of the slow-fast analysis in chart  $\bar{\varepsilon} = 1$ . Then we study the chart  $\bar{y} = 1$  by introducing  $\hat{\varepsilon} = y^{-1}\varepsilon = \hat{y}^{-1}$ . Due to (3.17) the critical manifold loses hyperbolicity at an exponential rate in this chart. To deal with this loss of hyperbolicity we proceed as in section 2 and extend the phase space dimension by introducing

$$q = e^{-2\hat{\varepsilon}^{-1}}, \quad (3.18)$$

as a new dynamic variable. We then blowup the singularity  $(q, \hat{\varepsilon}, x) = 0$  to a sphere using a weighted blowup and study the slow manifold near this sphere using desingularization and three different directional charts. We illustrate the geometry in Fig. 4. The blowup allows us to extend  $S_a$  (blue in Fig. 4) onto the blowup sphere (green in Fig. 4) and connect  $S_a$  with the visible fold of the PWS system. This in turn help us guide Fenichel's slow manifold  $S_{a,\varepsilon}$  (red in Fig. 4) up until the section  $x = \theta$ . In Appendix B we show that the result in Theorem 3.4 is in agreement with the result obtained by integrating the equations directly.





$$\begin{aligned}\dot{x} &= 1, \\ \varepsilon \dot{y} &= 2x + \frac{1 - \tanh(\hat{y})}{1 + \tanh(\hat{y})} = 2x + e^{-2\hat{y}}.\end{aligned}$$

In accordance with Theorem 3.2, this system possesses an attracting critical manifold  $S_a$  as a graph over  $\Sigma_{sl}$ . By Fenichel's theory compact subsets of this manifold perturbs to an invariant slow manifold  $S_{a,\varepsilon}$  for  $\varepsilon$  sufficiently small. A simple computation shows the following:

**Lemma 3.5.** *For  $\varepsilon \ll 1$  the attracting slow manifold  $S_{a,\varepsilon}$  intersects  $\hat{y} = \xi^{-1}$ , with  $\xi$  small but fixed, in  $(x_\xi(\varepsilon), \xi^{-1})$  with*

$$x_\xi(\varepsilon) = -\frac{1}{2}e^{-2\xi^{-1}} + \frac{\varepsilon}{2}e^{2\xi^{-1}} + \mathcal{O}(\varepsilon^2). \quad (3.19)$$

*Proof.* The critical manifold intersects  $y = \xi^{-1}$  in  $(x_\xi(0), \xi^{-1})$ . Since  $S_{a,\varepsilon}$  is  $\mathcal{O}(\varepsilon)$ -smoothly-close to  $S_a$  the result follows from a simple computation.  $\square$

By (3.14)  $x$  increases on  $S_a$  and therefore also on  $S_{a,\varepsilon}$  for  $\varepsilon \ll 1$ . We continue  $S_{a,\varepsilon}$  near  $\hat{y} = \infty$  by considering the chart  $\bar{y} = 1$ .

3.5. **Chart  $\bar{y} = 1$ .** In this chart we consider  $\hat{\varepsilon} = y^{-1}\varepsilon$  and obtain the following system of equations

$$\begin{aligned}\dot{x} &= \varepsilon, \\ \dot{y} &= \varepsilon \left( 2x + e^{-2\hat{\varepsilon}^{-1}} \right), \\ \dot{\hat{\varepsilon}} &= -\hat{\varepsilon}^2 \left( 2x + e^{-2\hat{\varepsilon}^{-1}} \right).\end{aligned}\tag{3.20}$$



The critical manifold from chart  $\bar{\varepsilon} = 1$  becomes

$$x = -\frac{1}{2}e^{-2\hat{\varepsilon}^{-1}}. \quad (3.21)$$

Setting  $\varepsilon = 0$  in (3.20) gives a new layer problem:

$$\begin{aligned} \dot{x} &= 0, \\ \dot{y} &= 0, \\ \dot{\hat{\varepsilon}} &= -\hat{\varepsilon}^2 \left( 2x + e^{-2\hat{\varepsilon}^{-1}} \right), \end{aligned} \quad (3.22)$$

in which (3.21) becomes a set of fix-points. In agreement with the analysis in chart  $\bar{\varepsilon} = 1$  this set is attracting for  $x < 0$  but it loses hyperbolicity at  $(x, y, \hat{\varepsilon}) = (0, 0, 0)$  at an exponential rate. Indeed, the linearization of (3.22) about (3.21) gives an eigenvalue

$$-2e^{-2\hat{\varepsilon}^{-1}}.$$

We then introduce  $q$  as in (3.18) and consider the extended system:

$$\begin{aligned} \dot{x} &= \varepsilon, \\ \dot{y} &= \varepsilon(2x + q), \\ \dot{\hat{\varepsilon}} &= -\hat{\varepsilon}^2(2x + q), \\ \dot{q} &= -2q(2x + q). \end{aligned} \quad (3.23)$$

This system is obtained by differentiation of (3.18):

$$\dot{q} = 2e^{-2\hat{\varepsilon}^{-1}}\hat{\varepsilon}^{-2}\dot{\hat{\varepsilon}} = 2q\hat{\varepsilon}^{-2}\dot{\hat{\varepsilon}}.$$

and using (3.18) in (3.20). The set

$$Q : \quad q = e^{-2\hat{\varepsilon}^{-1}}, \quad (3.24)$$

obtained from (3.18) is then by construction an invariant set of (3.23). However, it is implicit in (3.23) and we will evoke this invariance only when needed.

The half-plane

$$y \geq 0, \hat{\varepsilon} \geq 0, x = 0, \hat{\varepsilon} = 0, q = 0, \varepsilon = 0, \quad (3.25)$$

is a set of nonhyperbolic critical points of (3.23). We therefore consider the following blowup:

$$x = \bar{r}\bar{x}, \varepsilon = \bar{r}^2\bar{\varepsilon}, q = \bar{r}\bar{q} \quad (3.26)$$

The blowup transformation (3.26) gives rise to a vector-field  $\bar{X}$  on

$$(y, \hat{\varepsilon}, \bar{r}, (\bar{x}, \bar{\varepsilon}, \bar{q})) \in \bar{\mathbb{R}}_+^2 \times \bar{\mathbb{R}}_+ \times S^2.$$

Here  $\bar{X}|_{\bar{r}=0} = 0$  but the weights of  $r$  in the blowup in (3.26) are chosen so that  $\bar{r}^{-1}\bar{X}|_{\bar{r}=0}$  is nontrivial. It is  $\bar{r}^{-1}\bar{X}$  that we shall study in the following. We do so by considering the following charts:

$$\kappa_1 : \quad \bar{q} = 1 : \quad x = r_1x_1, \varepsilon = r_1^2\epsilon_1, q = r_1, \quad (3.27)$$

$$\kappa_2 : \quad \bar{\varepsilon} = 1 : \quad x = r_2x_2, \varepsilon = r_2^2\epsilon_2, q = r_2q_2, \quad (3.28)$$

and

$$\kappa_3 : \quad \bar{x} = 1 : \quad x = r_3, \varepsilon = r_3^2\epsilon_3, q = r_3q_3. \quad (3.29)$$



Notice that  $y$  and  $\hat{\varepsilon}$  are not transformed by this blowup transformation and we therefore keep using these symbols in the different charts. Geometrically, the half-plane of critical points (3.25) is upon (3.26) blown up to a cylinder  $\overline{\mathbb{R}}_+^2 \times S^2$ . In the following sections we analyze the different charts  $\kappa_1$ ,  $\kappa_2$  and  $\kappa_3$ .

**3.6. Chart  $\kappa_1$ .** Inserting (3.27) into (3.23) gives the following equations:

$$\begin{aligned} \dot{r}_1 &= -2r_1(2x_1 + 1), \\ \dot{x}_1 &= \epsilon_1 + 2x_1(2x_1 + 1), \\ \dot{y} &= \varepsilon(2x_1 + 1), \\ \dot{\hat{\varepsilon}} &= -\hat{\varepsilon}^2(2x_1 + 1), \\ \dot{\epsilon}_1 &= 4\epsilon_1(2x_1 + 1), \end{aligned} \tag{3.30}$$

after desingularization through division of the right hand side by  $r_1$ . Let

$$\rho(\xi) = e^{-2\xi^{-1}}. \tag{3.31}$$

Then  $\hat{\varepsilon} = \xi$  corresponds to  $r_1 = \rho(\xi)$  cf. (3.18).

We consider the following set

$$U_1 = \left\{ (r_1, x_1, y, \hat{\varepsilon}, \epsilon_1) \mid r_1 \in [0, \rho(\xi)], \hat{\varepsilon} \in [0, \xi], \right. \\ \left. y \in [0, \chi^{-1}], x_1 \in [-\chi^{-1}, \chi^{-1}] \right\},$$

with  $\xi$  and  $\chi$  positive but small and fixed. The critical manifold  $S_a$  from above becomes

$$S_{a,1} : \quad x_1 = -\frac{1}{2}, \quad y = 0, \quad \hat{\varepsilon} > 0.$$

The set (3.24) becomes

$$Q_1 : \quad r_1 = e^{-2\hat{\varepsilon}^{-1}}. \tag{3.32}$$

Since  $\varepsilon = r_1^2 \epsilon_1$  the system (3.30) possesses another invariant:

$$E_1 : \quad \varepsilon = r_1^2 \epsilon_1.$$

The advantage of the blowup method is that we have gained hyperbolicity of  $S_{a,1}$  for  $r_1 = \epsilon_1 = 0$ . Indeed, we have the following:

**Lemma 3.6.** *Within  $U_1$  there exists an attracting center manifold:*

$$M_{a,1} : \quad x_1 = -\frac{1}{2} + \frac{1}{2}\epsilon_1(1 + \mathcal{O}(\epsilon_1)).$$

*The manifold  $M_{a,1}$  contains  $S_{a,1}$  within  $y = 0$ ,  $\epsilon_1 = 0$  as a set of fix points. The center sub-manifold*

$$C_1 : \quad x_1 = -\frac{1}{2} + \frac{1}{2}\epsilon_1(1 + \mathcal{O}(\epsilon_1)), \quad r_1 = 0, \quad \hat{\varepsilon} = 0, \quad y = 0.$$

*is unique as a center manifold contained within  $r_1 = 0$ ,  $y = 0$ ,  $\hat{\varepsilon} = 0$ .*

*Proof.* This follows from straightforward computations. The manifold  $C_1$  is unique since it is overflowing.  $\square$



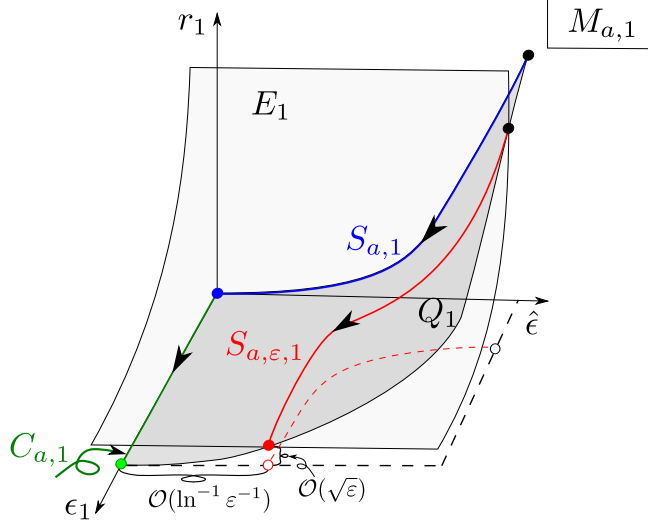


FIGURE 5. The reduced flow within  $M_{a,1}$ . The intersection of  $M_{a,1}$  with  $Q_1$  and  $E_1$  provides an extension of the Fenichel slow manifold up to  $\hat{\epsilon} = \mathcal{O}(\ln^{-1} \epsilon^{-1})$ .

**Remark 3.7.** The set  $M_{a,1} \cap Q_1 \cap E_1$  is  $\mathcal{O}(e^{-c/\epsilon})$ -close to  $S_{a,\epsilon}$  at  $r_1 = \rho(\xi)$ . Notice also that  $\epsilon_1 = \nu$  corresponds to  $r_1 = \sqrt{\epsilon\nu^{-1}}$  within  $E_1$ . Further restriction to  $Q_1$  gives  $\hat{\epsilon} = \mathcal{O}(\ln^{-1} \epsilon^{-1})$ . The manifold  $M_{a,1} \cap Q_1 \cap E_1$  is therefore the continuation  $S_{a,\epsilon,1}$  of Fenichel's slow manifold  $S_{a,\epsilon}$  up to  $\hat{\epsilon} = \mathcal{O}(\ln^{-1} \epsilon^{-1})$ . We illustrate the geometry in Fig. 5.

In this particular case, note that the expression for  $M_{a,1}$  is in agreement with (3.5) using (3.26). In fact, this expression can be taken to be independent of  $r_1$ . Since  $C_{a,1}$  is unique this allows us to select a unique  $M_{a,1}$  and therefore a unique  $S_{a,\epsilon,1}$ . We shall apply this selection henceforth.

On  $M_{a,1}$  we obtain the following reduced problem

$$\begin{aligned} \dot{r}_1 &= -2r_1, \\ \dot{y} &= \epsilon, \\ \dot{\hat{\epsilon}} &= -\hat{\epsilon}^2, \\ \dot{\epsilon}_1 &= 4\epsilon_1, \end{aligned} \tag{3.33}$$

after division by  $\epsilon_1(1 + \mathcal{O}(\epsilon_1))$ . This division desingularizes the dynamics within  $S_{a,1}$ , just as the passage to the fast time desingularized the dynamics within the critical manifold.

We describe (3.33) in the following lemma:

**Lemma 3.8.** Consider the reduced problem (3.33) on  $M_1$  and the mapping

$$P_1 : (y, \hat{\epsilon}, \epsilon_1) \mapsto (r_1^+, y^+, \hat{\epsilon}^+),$$



from  $\{(r_1, y, \hat{\varepsilon}, \epsilon_1) | r_1 = \rho(\xi)\}$  to  $\{(r_1, y, \hat{\varepsilon}, \epsilon_1) | \epsilon_1 = \nu\}$  obtained by the forward flow. Then

$$P_1(\varepsilon\xi^{-1}, \xi, \rho(\xi)^{-2}\varepsilon) = \begin{pmatrix} \sqrt{\varepsilon\nu^{-1}} \\ \frac{1}{4}\varepsilon \ln(\nu\varepsilon^{-1}) \\ 4\ln^{-1}(\nu\varepsilon^{-1}) \end{pmatrix} \quad (3.34)$$

In particular, the image  $P_1(\varepsilon\xi^{-1}, \xi, \rho(\xi)^{-2}\varepsilon)$  converges to the intersection

$$C_1 \cap \{\epsilon_1 = \nu\} : \quad r_1 = 0, y = 0, \hat{\varepsilon} = 0, x_1 = -\frac{1}{2} + \frac{1}{2}\nu(1 + \mathcal{O}(\nu)), \epsilon_1 = \nu, \quad (3.35)$$

as  $\varepsilon \rightarrow 0$ .

*Proof.* From the  $r_1$ - and the  $\epsilon_1$ -equation we obtain a travel time of  $T = \frac{1}{4} \ln(\rho^2\nu\varepsilon^{-1})$ . Integrating the  $y$ -equation then gives

$$y(T) = \varepsilon\xi^{-1} + \varepsilon T = \varepsilon \left( \xi^{-1} + \frac{1}{4} \ln(\rho^2\nu\varepsilon^{-1}) \right).$$

Using (3.31) this then simplifies to

$$\frac{1}{4}\varepsilon \ln(\nu\varepsilon^{-1}).$$

Finally, since  $\hat{\varepsilon} = y^{-1}\varepsilon$  we also obtain the final component of  $P_1$ .  $\square$

We continue the point (3.34) forward in time by moving to chart  $\kappa_2$ . The coordinate change between  $\kappa_1$  and  $\kappa_2$  is easily obtained from (3.27) and (3.28). It is given as

$$q_2 = 1/\sqrt{\epsilon_1}, \quad x_2 = x_1/\sqrt{\epsilon_1}, \quad r_2 = r_1\sqrt{\epsilon_1}, \quad (3.36)$$

valid for  $\epsilon_1 > 0$ .

**3.7. Chart  $\kappa_2$ .** Inserting (3.28) into (3.23) gives

$$\begin{aligned} \dot{x}_2 &= 1, \\ \dot{y} &= \varepsilon(2x_2 + q_2), \\ \dot{\hat{\varepsilon}} &= -\hat{\varepsilon}^2(2x_2 + q_2), \\ \dot{q}_2 &= -2q_2(2x_2 + q_2), \\ \dot{r}_2 &= 0, \end{aligned} \quad (3.37)$$

after division by  $r_2$ . In chart  $\kappa_2$  the point (3.34), using (3.36), becomes:

$$\begin{aligned} y &= \frac{1}{4}\varepsilon \ln(\nu\varepsilon^{-1}), \quad \hat{\varepsilon} = 4\ln^{-1}(\nu\varepsilon^{-1}), \\ x_2 &= \nu^{-1/2} \left( -\frac{1}{2} + \frac{1}{2}\nu(1 + \mathcal{O}(\nu)) \right), \quad q_2 = \nu^{-1/2}, \end{aligned} \quad (3.38)$$

and  $r_2 = \sqrt{\varepsilon}$ . In particular, (3.35) becomes

$$x_2 = \nu^{-1/2} \left( -\frac{1}{4} + \nu(1 + \mathcal{O}(\nu)) \right), \quad q_2 = \nu^{-1/2},$$

contained within  $r_2 = 0, y = 0, \hat{\varepsilon} = 0$ . We therefore consider  $r_2 = 0, y = 0, \hat{\varepsilon} = 0$  and obtain the following system

$$\frac{dq_2}{dx_2} = -2q_2(2x_2 + q_2),$$



upon elimination of time. The solution

$$q_2 = m_2(x_2) \equiv \frac{2e^{-2x_2^2}}{\sqrt{2\pi}(1 + \operatorname{erf}(\sqrt{2}x_2))}, \quad (3.39)$$

with

$$\operatorname{erf}(u) = \frac{2}{\sqrt{\pi}} \int_0^u e^{-s^2} ds,$$

corresponds to  $C_2 = \kappa_{21}(C_1)$ , and it intersects  $x_2 = \eta^{-1/2}$  in

$$r_2 = 0, y = 0, \hat{\varepsilon} = 0, x_2 = \eta^{-1/2}, q_2 = m_2(\eta^{-1/2}). \quad (3.40)$$

Hence, we obtain

**Proposition 3.9.** *The manifold  $M_2 \equiv \kappa_{21}(M_1)$  intersects  $x_2 = \eta^{-1/2}$  with*

$$q_2 = m_2(\eta^{-1/2}), \quad (3.41)$$

$$y = \frac{1}{4}\varepsilon \ln \varepsilon^{-1} + \varepsilon \left( \eta^{-1} + \frac{1}{2} \ln \left( \frac{\sqrt{2\pi}}{2} \left( 1 + \operatorname{erf}(\sqrt{2\eta^{-1}}) \right) \right) \right). \quad (3.42)$$

*Proof.* The expression (3.41) follows directly from (3.40) and since (3.37) is independent of  $r_2$ . To obtain (3.42) we consider

$$\frac{dy}{dx_2} = \varepsilon(2x_2 + m(x_2)), \quad (3.43)$$

obtained by inserting (3.41) into (3.37). We can then integrate (3.43) from

$$x_2 = x_{20} \equiv m_2^{-1}(\nu^{-1/2}),$$

to  $x_2 = \eta^{-1/2}$ . For this we use the fact that

$$\int m_2(x_2) dx_2 = \ln(1 + \operatorname{erf}(\sqrt{2}x_2)) - \ln \frac{2}{\sqrt{2\pi}} = \ln \frac{e^{-2x_2^2}}{m_2(x_2)}, \quad (3.44)$$

where we in the last equality have used Eq. (3.39). Therefore

$$\begin{aligned} y &= \frac{1}{4}\varepsilon \ln(\nu\varepsilon^{-1}) + \varepsilon(\eta^{-1} - x_{20}^2) + \frac{\varepsilon}{2} \left( \ln \frac{e^{-2\eta^{-1}}}{m_2(\eta^{-1/2})} - \ln \frac{e^{-2x_{20}^2}}{\nu^{-1/2}} \right) \\ &= \frac{1}{4}\varepsilon \ln \varepsilon^{-1} + \varepsilon\eta^{-1} + \frac{\varepsilon}{2} \ln \frac{e^{-2\eta^{-1}}}{m_2(\eta^{-1/2})}, \end{aligned}$$

using the initial condition from (3.38) and the second equation in (3.44). Using (3.39) we then obtain the expression in (3.42).  $\square$

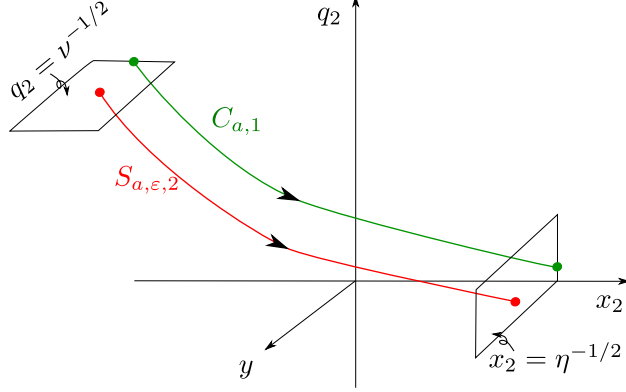
**Remark 3.10.** *In a more general setting, in which  $M_{a,2}$  is not independent of  $r_2$ , then one would have to apply regular perturbation theory in this chart. This would give rise  $\mathcal{O}(r_2)$ -terms in (3.41) and (3.42).*

We illustrate the dynamics in Fig. 6. Finally, we move to chart  $\kappa_3$ . Cf. (3.28) and (3.29) the coordinate change between the charts  $\kappa_2$  and  $\kappa_3$  is given as

$$q_3 = x_2^{-1}q_2, \quad r_3 = r_2x_2, \quad \varepsilon_3 = x_2^{-2}, \quad (3.45)$$

valid for  $x_2 > 0$ .



FIGURE 6. The dynamics within chart  $\kappa_2$ .

3.8. **Chart  $\kappa_3$ .** Inserting (3.28) into (3.23) gives

$$\begin{aligned} \dot{r}_3 &= r_3 \epsilon_3, \\ \dot{y} &= \varepsilon (2 + q_3), \\ \dot{\hat{\varepsilon}} &= -\hat{\varepsilon}^2 (2 + q_3), \\ \dot{q}_3 &= -q_3 (2(2 + q_3) + \epsilon_3), \\ \dot{\epsilon}_3 &= -2\epsilon_3^2, \end{aligned} \tag{3.46}$$

after desingularization through division of the right hand side by  $r_3$ . We consider the following set:

$$U_3 = \left\{ (r_3, y, \hat{\varepsilon}, q_3, \epsilon_3) \mid r_3 \in [0, \theta], y \in [0, \theta^{-1}], \right. \\ \left. \hat{\varepsilon} \in [0, \xi], \epsilon_3 \in [0, \eta] \right\}.$$

The point (3.40) becomes

$$r_3 = 0, y = 0, \hat{\varepsilon} = 0, q_3 = \eta^{1/2} m_2(\eta^{-1/2}), \epsilon_3 = \eta, \tag{3.47}$$

using the coordinate transformation in (3.45). Here:

$$N_3 : \quad q_3 = 0,$$

is an attracting (but inflowing and non-unique) center manifold. We use Fenichel's normal form to straighten out the stable fibers:

**Proposition 3.11.** *For  $\varepsilon$  sufficiently small, there exists a smooth transformation  $(r_3, y, \epsilon_3) \mapsto (r_3, \tilde{y}, \epsilon_3)$  within  $U_3$ :*

$$y = \tilde{y} + \varepsilon \left( -\frac{1}{2} \ln \left( 1 + \frac{q_3}{2} S_3(\epsilon_3) \right) \right), \tag{3.48}$$



with

$$S_3(\epsilon_3) = \sqrt{2\pi\epsilon_3^{-1}}e^{2\epsilon_3^{-1}} \left(1 - \operatorname{erf} \left(\sqrt{2\epsilon_3^{-1}}\right)\right) = 1 + \mathcal{O}(\epsilon_3), \quad (3.49)$$

transforming (3.46) into:

$$\dot{r}_3 = r_3\epsilon_3, \quad (3.50)$$

$$\dot{y} = 2\varepsilon,$$

$$\dot{\epsilon} = -2\epsilon^2,$$

$$\dot{q}_3 = -2q_3(2(2+q_3) + \epsilon_3),$$

$$\dot{\epsilon}_3 = -2\epsilon_3^2. \quad (3.51)$$

*Proof.* The existence of the transformation follows from Fenichel's normal form [13]. The expression in (3.48) follows by considering the  $r_3 = 0$  system:

$$\dot{y} = \varepsilon(2 + q_3),$$

$$\dot{q}_3 = -q_3(2(2 + q_3) + \epsilon_3),$$

$$\dot{\epsilon}_3 = -2\epsilon_3^2,$$

and applying a transformation  $y = \tilde{y} + \varepsilon W(q_3, \epsilon_3)$  with  $W$  having the property that

$$\dot{\tilde{y}} = 2\varepsilon.$$

This gives rise to the following equation for  $W(q_3, \epsilon_3)$

$$q_3 = \partial_{q_3} W \dot{q}_3 + \partial_{\epsilon_3} W \dot{\epsilon}_3.$$

Using the method of characteristic we obtain a solution

$$W = -\frac{1}{2} \ln \left(1 + \frac{q_3}{2} S_3(\epsilon_3)\right). \quad (3.52)$$

The smoothness of  $S_3$  and the expansion in (3.49) follows from the following asymptotics of  $\operatorname{erf}(u)$  for  $u \rightarrow \infty$ :

$$\operatorname{erf}(u) = 1 - \frac{e^{-u^2}}{\sqrt{\pi}u} (1 + \mathcal{O}(u^{-2})).$$

□

Using (3.45) we can write (3.52) as

$$W = -\frac{1}{2} \ln \left(1 + \frac{x_2^{-1} q_2}{2} S_3(x_2^{-2})\right).$$

In particular for  $q_2 = m_2(x_2)$  with  $m_2$  as in (3.39)

$$W = -\frac{1}{2} \ln \left(1 + \frac{1 - \operatorname{erf}(\sqrt{2}x_2)}{1 + \operatorname{erf}(\sqrt{2}x_2)}\right) = -\frac{1}{2} \ln \frac{2}{\operatorname{erf}(\sqrt{2}x_2) + 1}.$$



Therefore (3.42) becomes

$$\begin{aligned}\tilde{y} &= \frac{1}{4}\varepsilon \ln \varepsilon^{-1} + \varepsilon \left( \eta^{-1} + \frac{1}{2} \ln \left( \frac{\sqrt{2\pi}}{2} (1 + \operatorname{erf}(\sqrt{2\eta^{-1}})) \right) \right. \\ &\quad \left. + \frac{1}{2} \ln \frac{2}{1 + \operatorname{erf}(\sqrt{2\eta^{-1}})} \right) \\ &= \frac{1}{4}\varepsilon \ln \varepsilon^{-1} + \varepsilon \left( \eta^{-1} + \frac{1}{4} \ln(2\pi) \right),\end{aligned}\tag{3.53}$$

in terms of  $\tilde{y}$ .

**Lemma 3.12.** *Consider the reduced problem (3.50)<sub>q3=0</sub> on  $N_3$  and the mapping*

$$P_3 : (r_3, \tilde{y}, \hat{\varepsilon}) \mapsto (\tilde{y}^+, \hat{\varepsilon}^+, \epsilon_3^+)$$

*from  $\{(r_3, \tilde{y}, \hat{\varepsilon}, \epsilon_3) | \epsilon_3 = \eta\}$  to  $\{(r_3, \tilde{y}, \hat{\varepsilon}, \epsilon_3) | r_3 = \theta\}$  obtained by the forward flow. Then*

$$P_3(\sqrt{\varepsilon\eta^{-1}}, \tilde{y}, \tilde{y}^{-1}\varepsilon) = \begin{pmatrix} \tilde{y} + \theta^2 - \varepsilon\eta^{-1} \\ (\tilde{y} + \theta^2 - \varepsilon\eta^{-1})^{-1}\varepsilon \\ \varepsilon\theta^{-2} \end{pmatrix}$$

*Proof.* To solve (3.50) we initially decouple the  $\hat{\varepsilon}$ -equation and consider

$$\begin{aligned}\dot{r}_3 &= 2r_3, \\ \dot{\tilde{y}} &= 4r_3^2 = 2r_3\dot{r}_3 = \frac{dr_3^2}{dt}, \\ \dot{\epsilon}_3 &= -4\epsilon_3,\end{aligned}$$

obtained after division of  $\frac{1}{2}\epsilon_3$ . Then with initial conditions:

$$r_3(0) = \sqrt{\varepsilon\eta^{-1}}, \quad \epsilon_3(0) = \eta,$$

and  $r_3(T) = \theta$ ,  $\epsilon_3(T) = \varepsilon\theta^{-2}$  we obtain a travel time of  $T = \frac{1}{2} \ln(\theta\sqrt{\nu\varepsilon^{-1}})$ . Therefore

$$\tilde{y}(T) = \tilde{y}(0) + r_3(T)^2 - r_3(0)^2 = y(0) + \theta^2 - \varepsilon\eta^{-1},$$

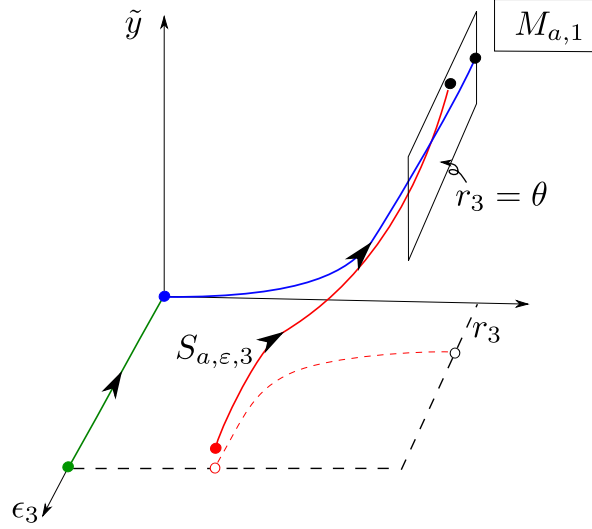
which completes the proof. □

Finally, applying  $P_3$  to the initial condition (3.53) we conclude using (3.48) and  $q_3(T) = \mathcal{O}(e^{-c/\varepsilon})$  that the slow manifold intersects  $r_3 = \theta$  in

$$\begin{aligned}y &= \theta^2 + \frac{1}{4}\varepsilon \ln \varepsilon^{-1} + \frac{1}{4}\varepsilon \left( \ln \frac{\pi}{2} + R(\sqrt{\varepsilon}) \right) \\ &= \theta^2 + \varepsilon \left( \frac{1}{4} \ln \left( \frac{\pi}{2} \varepsilon^{-1} \right) + R(\sqrt{\varepsilon}) \right),\end{aligned}$$

with  $R(\sqrt{\varepsilon}) = \mathcal{O}(e^{-c\varepsilon^{-1}})$  smooth. We illustrate the geometry in Fig. 7. This completes the proof of Theorem 3.4.



FIGURE 7. The dynamics within chart  $\kappa_3$ .

#### 4. A FLAT SLOW MANIFOLD IN A MODEL FOR AIRCRAFT GROUND DYNAMICS

In this section we consider the system (1.6), repeated here for convinience:

$$\begin{aligned}\dot{u} &= \varepsilon(\alpha - v), \\ \dot{v} &= u + (v - a)e^{vb},\end{aligned}\tag{4.1}$$

with parameters  $a$  and  $b$  fixed and use  $\alpha$  as a bifurcation parameter. In comparison with [31] we have replaced  $b$  by  $b^{-1}$ . The system (4.1) possesses a critical manifold which is a graph over the fast variable  $v$ :

$$C = \{(u, v) | u = (a - v)e^{vb}\}.$$

Linearization (4.1) about  $C$  for  $\varepsilon = 0$  gives

$$-(1 + b(v - a))e^{vb},\tag{4.2}$$

as a single non-trivial eigenvalue. The manifold  $C$  therefore splits into an attracting critical manifold:<sup>1</sup>

$$\hat{S} = C \cap \{v > a - b^{-1}\},$$

a fold point:

$$F = (u_f, v_f),$$

with

$$u_f = b^{-1}e^{(a-b^{-1})b}, \quad v_f = a - b^{-1},$$

and a repelling critical manifold:

$$S = C \cap \{v < a - b^{-1}\},$$

<sup>1</sup>Here we do not use  $S_a$  and  $S_r$  for attracting and repelling critical manifolds because we find that this becomes confusing when we later reverse the direction of time.



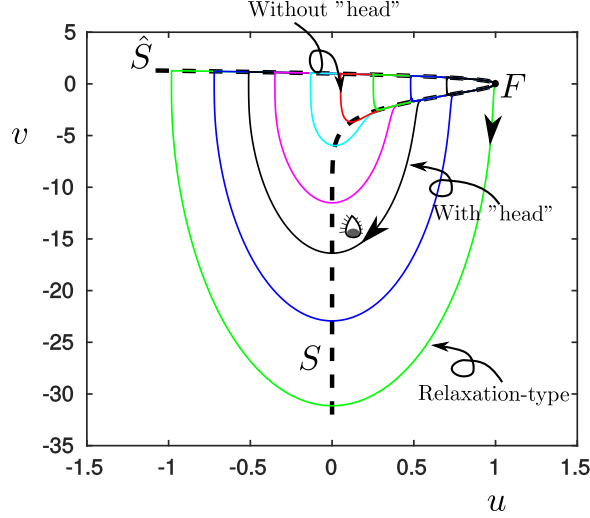


FIGURE 8. Different limit cycles: without head, with head and relaxation-type oscillations, near the canard explosion for  $a = b = 1$ ,  $\varepsilon = 10^{-3}$  and  $\alpha \approx -10^{-3}$ .

Compact subsets of  $\hat{S}$  and  $S$  perturb by Fenichel's theory to  $\hat{S}_\varepsilon$  and  $S_\varepsilon$ . The system undergoes a Hopf bifurcation near the fold  $F$  at a parameter value  $\alpha = \alpha_H \equiv a - b^{-1} + \mathcal{O}(\varepsilon)$  which leads to the a canard explosion phenomenon near the canard value  $\alpha_c \equiv a - b^{-1} + \mathcal{O}(\varepsilon)$  where the limit cycles born in the Hopf bifurcation undergoes  $\mathcal{O}(1)$ -changes within parameter regime of width  $\mathcal{O}(e^{-c/\varepsilon})$ ,  $c > 0$ . See [25]. Examples of limit cycles are shown in Fig. 8 near  $\alpha_c \approx -10^{-3}$  for  $a = b = 1$  and  $\varepsilon = 10^{-3}$ . The small limit cycles, following the repelling manifold  $S_\varepsilon$  before jumping directly towards the attracting manifold  $\hat{S}_\varepsilon$ , are frequently called canard cycles *without head*. Similarly, the canard cycles that leave  $S_\varepsilon$  on the other side, escaping towards infinity  $v \rightarrow -\infty$  before returning to  $\hat{S}_\varepsilon$ , are said to be *with head*. Eventually the canard cycles become relaxation oscillations that escape directly towards infinity  $v \rightarrow -\infty$  at the fold  $F$ . Note how trajectories cross  $S$  for  $v \ll 0$ . This is due to the fact that  $S$  loses hyperbolicity at infinity  $v \rightarrow -\infty$ . Similar transition to relaxation oscillations occur in [2, Fig. 4] and [15], but in (4.1) the loss of hyperbolicity occurs at an exponential rate  $\mathcal{O}(e^{vb})$ . Therefore the classical theory of canard explosion [25] does not describe the transition from canard cycles without head to those with head. The aim of this section is to apply our approach to (4.1) and obtain a description of this transition that in turn establishes the existence of large canard cycles.

**4.1. Setup.** To obtain large amplitude limit cycles near the canard value, we proceed as in the classical analysis [25], and consider two sections at  $v = v_f$ :

$$\Gamma = \{(u, v) | u \in [-c^{-1}, c^{-1}], v = v_f\}, \quad (4.3)$$

$$\Lambda = \{(u, v) | u \in [-c^{-1} + u_f, c^{-1} + u_f], v = v_f\}, \quad (4.4)$$

for  $c$  sufficiently small. See Fig. 9. Let  $(u, v) \in \Gamma$  and consider the forward orbit



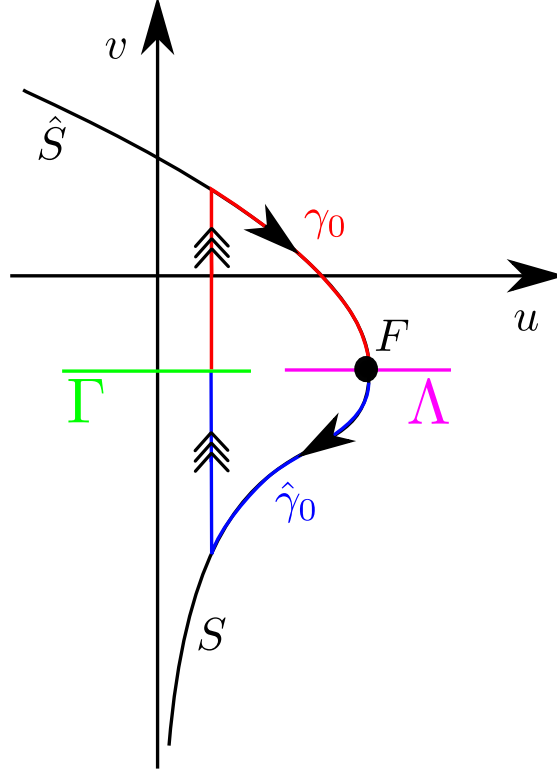


FIGURE 9. Illustration of the critical manifold  $C = M \cup \{F\} \cup S$  and the two sections  $\Gamma$  and  $\Lambda$ .

$\gamma_\varepsilon(u, \alpha)$  and backward orbit  $\hat{\gamma}_\varepsilon(u, \alpha)$ . Denote their intersection with  $\Lambda$  by  $d_\varepsilon(u, \alpha)$  and  $\hat{d}_\varepsilon(u, \alpha)$ , respectively. For  $u \geq \bar{c}^{-1} > 0$ , with  $\bar{c} > c$  fixed but large, the standard theory applies. Indeed, by the transverse intersection of (fixed copies of)  $M_\varepsilon$  and  $S_\varepsilon$  at  $\alpha = \alpha_c$  it is possible to solve  $d_\varepsilon(u, \alpha) = \hat{d}_\varepsilon(u, \alpha)$  for  $\alpha$  by the implicit function theorem. This argument fails near  $u = 0$ . In the following we will study  $S$  using our methods and describe the limit cycles that intersect  $\Gamma$  with  $u \approx 0$ . For this we reverse time so that  $S$  becomes attracting and consider the equations:

$$\begin{aligned} \dot{u} &= \varepsilon(\alpha - v), \\ \dot{v} &= u + (v - a)e^{vb}. \end{aligned} \tag{4.5}$$

**4.2. Equations at infinity.** To deal with loss of hyperbolicity for  $v \rightarrow -\infty$  we introduce the following “chart”:

$$x = -uv^{-1}, \quad y = -v^{-1}, \tag{4.6}$$

based upon Poincaré compactification. Then  $y = 0^+$  corresponds to  $v = -\infty$ . It is convenient if the fold  $F$  is visible in this chart (4.6) and we shall therefore henceforth assume that

$$v_f = a - b^{-1} < 0.$$



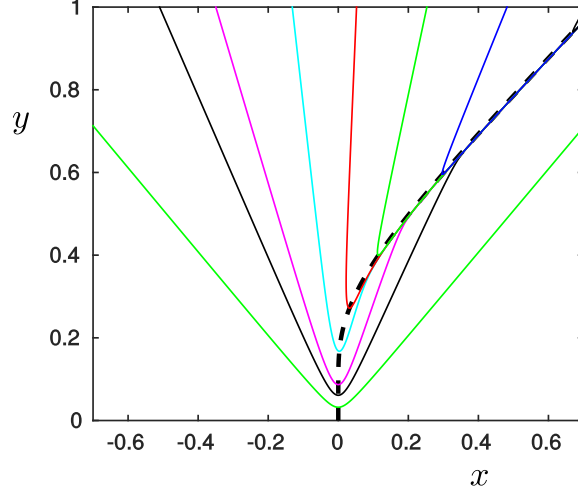


FIGURE 10. The limit cycles from Fig. 8 in the  $(x, y)$ -variables.

Using (4.5) and (4.6) we obtain the following equations:

$$\begin{aligned}\dot{x} &= \varepsilon(1 + \alpha y) + x \left( x - (1 + \alpha y)e^{-y^{-1}b} \right), \\ \dot{y} &= y \left( x - (1 + \alpha y)e^{-y^{-1}b} \right).\end{aligned}\tag{4.7}$$

The critical manifold  $S$  from above becomes

$$S: \quad x = (1 + \alpha y)e^{-y^{-1}b}, \quad y \in (0, y_f)$$

in the  $(x, y)$ -variables while the fold  $F$  becomes

$$F = (x_f, y_f).$$

Here  $x_f = -u_f v_f^{-1}$ ,  $y_f = -v_f^{-1}$ . We will continue to denote  $S$  and  $F$  by the same symbols in the new variables  $(x, y)$ . The set  $S$  is still a set of critical points of  $(4.7)_{\varepsilon=0}$ . But opposed to (4.5), where the fibers were vertical:  $\mathcal{F}_{w_0} = \{(w_0, z) | z \in \mathbb{R}\}$  for  $\varepsilon = 0$ , the singular fibers are now tilted:

$$\mathcal{F}_{w_0} = \{(x, y) | x = w_0 y\},$$

with respect to the  $(x, y)$ -variables. See also Fig. 10 where segments of the limit cycles in Fig. 8 are illustrated in the  $(x, y)$ -variables.

The fibers to the left of  $S$  all emanate from the unstable fibers of  $\hat{S}$  (which itself is only partially visible in the chart  $(x, y)$ ). Note again that  $S$  loses hyperbolicity at  $y = 0$  at an exponentially rate since the linearization of  $(4.7)_{\varepsilon=0}$  about  $S$  yields

$$-y^{-1}b e^{-y^{-1}b} (1 + v_f y).$$

The section  $\Gamma$  in (4.3) becomes

$$\Gamma = \{(x, y) | x \in [-\nu, \nu], y = y_f\},$$



with  $\nu = -c^{-1}v_f^{-1}$ , in the new variables. We again use the same symbol for this section.

**4.3. Main result.** By Fenichel's theory, the slow manifold  $S_\varepsilon$  intersects  $y = \delta$  in  $(x_\delta(\varepsilon), \delta)$  with

$$x_\delta(\varepsilon) \equiv (1 + a\delta)e^{-\delta^{-1}b} + \mathcal{O}(\varepsilon),$$

with  $\delta < y_f$ . We consider the following section

$$\Sigma = \{(x, y) | x \in [x_\delta(\varepsilon) - \nu, x_\delta(\varepsilon) + \nu], y = \delta\},$$

together with the following mapping

$$P_\varepsilon : \Gamma \rightarrow \Sigma,$$

obtained by the forward flow of (4.7). We will then prove the following:

**Theorem 4.1.** *Fix  $\nu$  sufficiently small. Then for  $\varepsilon$  sufficiently small, the mapping  $P_\varepsilon$  is a strong contraction, satisfying the following estimates*

$$P_\varepsilon(x) = x_\delta(\varepsilon) + \mathcal{O}(e^{-c/\varepsilon}), \quad P'_\varepsilon(x) = \mathcal{O}(e^{-c/\varepsilon}).$$

We will focus on the details of subsets of  $\Gamma$  with  $x = o(1)$  with respect to  $\varepsilon$ . For this we proceed as described in section 2 by introducing the following function

$$q = (1 + ay)e^{-y^{-1}b}, \quad (4.8)$$

as a new variable and consider the extended system:

$$\begin{aligned} \dot{x} &= y(\varepsilon(1 + ay) + x(x - q)), \\ \dot{y} &= y^2(x - q), \\ \dot{q} &= q(x - q) \left( b + \frac{ay}{1 + ay} \right). \end{aligned} \quad (4.9)$$

This system is obtained by differentiating (4.8) with respect to time and using (4.7) and (4.8) to eliminate the exponential  $e^{-y^{-1}b}$ . We have also multiplied the right hand side by  $y$ . This corresponds to a nonlinear transformation of time for  $y > 0$  which de-singularizes the system for  $y = 0$ . The set

$$Q : \quad q = (1 + ay)e^{-y^{-1}b}, \quad (4.10)$$

obtained from (4.8) is by construction an invariant set of (4.9). Again it is implicit in (4.9) and we can invoke it when needed. We could also have set  $q = e^{-y^{-1}b}$ , the analysis would be almost identical. However, some of the resulting expressions simplify using (4.8). In particular,  $S$  just reads:

$$S : \quad x = q. \quad (4.11)$$

The set  $S$  in (4.11) is a set of critical points of  $(4.8)_{\varepsilon=0}$ . It is nonhyperbolic for  $x = q = 0$ , but now the system is algebraic to leading order. To deal with this loss of hyperbolicity we may therefore consider the following blowup:

$$q = r\bar{q}, \quad x = r\bar{x}, \quad \varepsilon = r^2\bar{\varepsilon}, \quad r \geq 0, \quad (\bar{q}, \bar{x}, \bar{\varepsilon}) \in S^2, \quad (4.12)$$

together with the following charts:

$$\begin{aligned} \kappa_1 : \quad \bar{q} = 1 : \quad q &= r_1, \quad x = r_1x_1, \quad \varepsilon = r_1^2\varepsilon_1, \\ \kappa_2 : \quad \bar{\varepsilon} = 1 : \quad q &= r_2q_2, \quad x = r_2x_2, \quad \varepsilon = r_2^2. \end{aligned}$$



Notice that  $y$  is not part of the transformation (4.12) so geometrically  $x = q = \varepsilon = 0$  is blown-up to a cylinder of spheres:  $(y, (\bar{q}, \bar{x}, \bar{\varepsilon})) \in \bar{\mathbb{R}}_+ \times S^2$ .

4.4. **Chart  $\kappa_1$ .** In this chart we obtain the following equations from (4.9)

$$\begin{aligned} \dot{r}_1 &= r_1(x_1 - 1) \left( b + \frac{ay}{1 + ay} \right), \\ \dot{x}_1 &= -x_1(x_1 - 1) \left( b + \frac{ay}{1 + ay} + y \right) + y\epsilon_1(1 + \alpha y), \\ \dot{y} &= y^2(x_1 - 1), \\ \dot{\epsilon}_1 &= -2\epsilon_1(x_1 - 1) \left( b + \frac{ay}{1 + ay} \right), \end{aligned} \quad (4.13)$$

after division by  $r_1$ . In this chart the invariant set  $Q$  in (4.10) becomes:

$$Q_1 : \quad r_1 = (1 + ay)e^{-y^{-1}b}.$$

The hyperbolas

$$E_1 : \quad \varepsilon = r_1^2 \epsilon_1,$$

are also invariant. We consider the following set:

$$U_1 = \left\{ (r_1, x_1, y, \epsilon_1) \mid \begin{aligned} \epsilon_1 &\in [0, \mu^{-1}], \\ x_1 &\in [-\xi^{-1}, \xi^{-1}], \\ r_1 &\in [0, \rho(\delta)], \\ y &\in [0, \delta] \end{aligned} \right\},$$

with  $\mu, \xi$  and  $\delta$  small but fixed with respect to  $\varepsilon$ . As always, the two planes  $\{\epsilon_1 = 0\}$  and  $\{r_1 = 0\}$  are invariant. Within the former we re-discover  $S$  from (4.11) as

$$S_1 : \quad x_1 = 1, r_1 = 0.$$

Using the blowup we have gained hyperbolicity of  $S$ . We have:

**Proposition 4.2.** *For  $\delta$  sufficiently small, the following holds: Within  $U_1$  there exists a center manifold:*

$$M_1 : \quad x_1 = 1 + m_1(y, \epsilon_1), \quad m_1(y, \epsilon_1) \equiv \epsilon_1 y (b + \mathcal{O}(y)), \quad (4.14)$$

which is foliated by the invariant sets  $E_1$  and  $Q_1$ . The manifold  $M_1$  contains  $S_1$  and

$$C_1 : \quad x_1 = 1, r_1 = 0, y = 0,$$

as manifolds of equilibria within  $\epsilon_1 = 0$  and  $r_1 = y = 0$ , respectively.

*Proof.* The set  $\{U_1 \mid x_1 = 1, y = 0\}$  is a set of equilibria. The linearization about a point in this set gives three zero eigenvalues and one non-zero  $\lambda = -b$ . The result then follows from standard center manifold theory.  $\square$

**Remark 4.3.** *Note here that the center manifold in chart  $\kappa_1$  is only truly local in  $y$ . In  $U_1$  we may take  $\epsilon_1$  large (but fixed with respect to  $\varepsilon$ ). Notice also that*

$$M_1 \cap E_1 \cap Q_1,$$



by Fenichel's theory, is  $\mathcal{O}(e^{-c/\varepsilon})$ -close to  $S_\varepsilon$  at  $r_1 = \rho(\delta)$ . We shall therefore view  $M_1 \cap E_1 \cap Q_1$  as the continuation of Fenichel's slow manifold  $S_\varepsilon$  into chart  $\kappa_1$  by the backward flow.

On  $M_1$  we obtain the following reduced system

$$\begin{aligned} \dot{r}_1 &= r_1, \\ \dot{y} &= y^2 \left( b + \frac{ay}{1+ay} \right)^{-1}, \\ \dot{\epsilon}_1 &= -2\epsilon_1, \end{aligned} \tag{4.15}$$

after division of  $m_1(y, \epsilon_1) \left( b + \frac{ay}{1+ay} \right) = \epsilon_1 y (1 + \mathcal{O}(y))$  which desingularizes the flow within  $\epsilon_1 = 0$  and  $y = 0$ .

The system (4.13) also has a 1D center manifold

$$D_1 : \quad r_1 = 0, x_1 = 0, \epsilon_1 = 0,$$

within  $U_1$ , which emanates from the equilibrium:

$$r_1 = 0, x_1 = 0, y = 0, \epsilon_1 = 0. \tag{4.16}$$

Indeed the linearization about (4.16) yields the following eigensolutions  $(\lambda_i, v_i)$

$$\begin{aligned} \lambda_1 &= -1, v_1 = (1, 0, 0, 0), \\ \lambda_2 &= 1, v_2 = (0, 1, 0, 0), \\ \lambda_3 &= 0, v_3 = (0, 0, 1, 0), \\ \lambda_4 &= 2, v_4 = (0, 0, 0, 1). \end{aligned}$$

Each eigenvector  $v_i$  is invariant. In particular  $W_{loc}^s(0) = \text{span } v_1$  and  $D_1 = \text{span } v_3$ .

We illustrate the dynamics within  $Q_1$  in Fig. 11 using a projection onto the  $(y, x_1, \epsilon_1)$ -space.

**Proposition 4.4.** *Consider the following interval of  $x_1$ -values:*

$$X = [-\xi\sqrt{\varepsilon}\ln^{-1}\varepsilon^{-1}, \xi\sqrt{\varepsilon}\ln^{-1}\varepsilon^{-1}].$$

*Then for  $\varepsilon$  sufficiently small the following holds: The mapping from*

$$\Lambda_1 \equiv \{U_1 | r_1 = \rho(\delta), x_1 \in X, y = \delta, \epsilon_1 = \varepsilon\rho(\delta)^{-2}\},$$

*to*

$$\Gamma_1 \equiv \{U_1 | \epsilon_1 = \mu^{-1}\},$$

*obtained by the forward flow of (4.13), is well-defined and the image values of  $r_1$  and  $x_1$ ,  $(r_1^+, x_1^+)(x_1)$ , satisfy:*

$$\begin{aligned} r_1^+(x_1) &= \sqrt{\varepsilon\mu}, \\ (x_1^+)(x_1) &= \sqrt{\mu}\rho(\delta)x_1/\sqrt{\varepsilon}(\tilde{\delta}_2\tau_2(\ln(\rho(\delta)/\sqrt{\mu\varepsilon}), \tilde{\delta}_2) + 1)(1 + \mathcal{O}(\sqrt{\varepsilon})), \\ (x_1^+)'(x_1) &= \mathcal{O}(\varepsilon^{-1/2}\ln\varepsilon^{-1}), \end{aligned} \tag{4.17}$$

*where*

$$\begin{aligned} \tilde{\delta}_2 &= \delta(1 + \mathcal{O}(x_1)), \\ \tau_2(t, \tilde{y}_0) &= bt + a \ln \frac{1 + \tilde{y}_0(a+t)}{1 + \tilde{y}_0a}. \end{aligned}$$

*and since  $r_1 = (1 + ay)e^{-y^{-1}b}$  we have  $y^+ = \ln^{-1}\varepsilon^{-1/2}(1 + o(1))$ .*



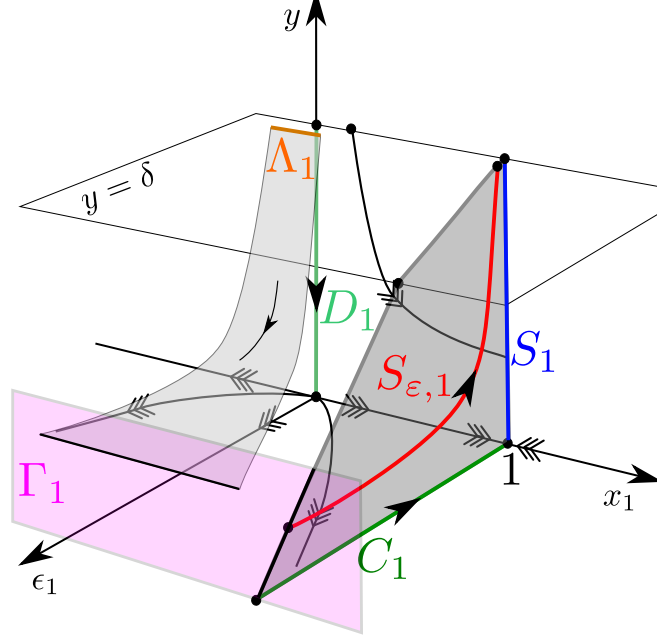


FIGURE 11. The dynamics within  $Q_1$  in  $\kappa_1$  using a projection onto the  $(y, x_1, \epsilon_1)$ -space.

*Proof.* We drop the subscripts in (4.15) and divide the right hand side by  $1 - x$ :

$$\begin{aligned} \dot{x} &= x \left( b + \frac{ay}{1+ay} + y \right) + y\epsilon \frac{1+\alpha y}{1-x}, \\ \dot{y} &= -y^2, \\ \dot{\epsilon} &= 2\epsilon \left( b + \frac{ay}{1+ay} \right). \end{aligned} \quad (4.18)$$

Here  $(x, y, \epsilon) = 0$  is a non-hyperbolic equilibrium: The eigenvalues of the linearization are  $1, 0, 2$ . We therefore consider the following blowup:

$$x = u\bar{x}, \quad \epsilon = u^2\bar{\epsilon}, \quad (u, (\bar{x}, \bar{\epsilon})) \in \bar{\mathbb{R}}_+ \times S^1, \quad (4.19)$$

and the following chart:

$$\bar{\epsilon} = 1 : \quad x = u_2x_2, \quad \epsilon = u_2^2.$$

Insertion gives:

$$\begin{aligned} \dot{x}_2 &= y \left( x_2 + u_2 \frac{1+\alpha y}{1-x} \right) \left( b + \frac{ay}{1+ay} \right)^{-1}, \\ \dot{y} &= -y^2 \left( b + \frac{ay}{1+ay} \right)^{-1}, \\ \dot{u}_2 &= u_2, \end{aligned} \quad (4.20)$$



after division of the right hand side by

$$b + \frac{ay}{1+ay} > 0.$$

We wish to describe the mapping from  $\{y = \delta\}$  to  $\{u_2 = \mu^{-1/2}\}$  obtained by the forward flow of (4.20) for initial conditions with  $x_2 \in [-\xi \ln^{-1} \varepsilon^{-1}, \xi \ln^{-1} \varepsilon^{-1}]$ . We will describe this mapping in terms of the variables introduced in the following lemma:

**Lemma 4.5.** *There exists a smooth transformation*

$$(x_2, y) = (\tilde{x}_2, \tilde{y}) + \mathcal{O}(\tilde{x}_2 \tilde{y} u_2),$$

that transforms (4.20) into

$$\begin{aligned} \dot{\tilde{x}}_2 &= \tilde{y} \tilde{x}_2 \left( b + \frac{a\tilde{y}}{1+a\tilde{y}} \right)^{-1}, \\ \dot{\tilde{y}} &= -\tilde{y}^2 \left( b + \frac{a\tilde{y}}{1+a\tilde{y}} \right)^{-1}, \\ \dot{u}_2 &= u_2. \end{aligned} \tag{4.21}$$

*Proof.* The transformation is just obtained by straightening out the unstable fibers.  $\square$

Consider the initial conditions  $(\tilde{x}_{20}, \tilde{y}_0, u_{20})$  with

$$u_{20} = \sqrt{\varepsilon} \rho(\delta)^{-1},$$

and

$$\tilde{y}_0 = \delta(1 + \mathcal{O}(x_{20} u_{20})),$$

using that  $y(0) = \delta$ . Then the solution of (4.21) is easily obtained:

$$\begin{aligned} \tilde{x}_2(t) &= \tilde{x}_{20}(1 + \tilde{y}_0 \tau_2(t, \tilde{y}_0)), \\ \tilde{y}(t) &= \frac{\tilde{y}_0}{1 + \tilde{y}_0 \tau_2(t, \tilde{y}_0)}, \\ u_2(t) &= \sqrt{\varepsilon} \rho(\delta)^{-1} e^t, \end{aligned}$$

where

$$\begin{aligned} \tau_2(t, \tilde{y}_0) &= \int_0^t \left( b + \frac{a\tilde{y}_0}{1 + \tilde{y}_0(a+s)} \right) ds \\ &= bt + a \ln \frac{1 + \tilde{y}_0(a+t)}{1 + \tilde{y}_0 a}. \end{aligned}$$

Setting  $u_2(T) = \mu^{-1/2}$  gives  $T = \ln(\rho(\delta)/(\sqrt{\mu\varepsilon}))$  and hence

$$\begin{aligned} \tilde{x}_2(T) &= \tilde{x}_{20}(\tilde{y}_0 \tau_2(\ln(\rho(\delta)/\sqrt{\mu\varepsilon}), \tilde{y}_0) + 1) \\ \tilde{y}(T) &= \frac{\tilde{y}_0}{1 + \tilde{y}_0 \tau_2(\ln(\rho(\delta)/\sqrt{\mu\varepsilon}), \tilde{y}_0)}. \end{aligned}$$

In terms of  $x_2$  we therefore obtain

$$x_2(T) = x_{20}(1 + \mathcal{O}(\tilde{y}_0 \sqrt{\varepsilon} \rho(\delta)^{-1}))(\tilde{y}_0 \tau_2(\ln(\rho(\delta)/\sqrt{\mu\varepsilon}), \tilde{y}_0) + 1).$$

Finally, we return to  $x$  (or  $x_1$ ) and  $y$  and obtain the expression in (4.17).  $\square$



Using the chart  $\bar{x} = 1$  of the blowup (4.19) it is possible to guide the set of initial conditions:

$$x_1 \in [\xi\sqrt{\varepsilon}\ln^{-1}\varepsilon^{-1}, \chi], \quad \chi < \nu,$$

within  $r_1 = \rho(\delta)$  towards  $\{x_1 = \nu\}$  for  $\nu$  sufficiently small, and eventually prove the statement of Theorem 4.1 for this set of initial conditions using the uniform contraction along  $M_1$ . Similarly, the set

$$x_1 \in [-\chi, -\xi\sqrt{\varepsilon}\ln^{-1}\varepsilon^{-1}], \quad (4.22)$$

can be guided towards  $\{x_1 = -\nu\}$  using the chart  $\bar{x} = -1$  of the blowup (4.19). From there this set can be continued using the chart  $\bar{x} = -1$  of (4.12). We skip the details because it is lengthy but, more importantly, because it is largely independent of the method promoted in this paper.

The image points described in Proposition 4.4 are continued into chart  $\kappa_2$  in the following section.

**4.5. Chart  $\kappa_2$ .** Insertion gives

$$\dot{x}_2 = y((1 + \alpha y) + x_2(x_2 - q_2)), \quad (4.23)$$

$$\dot{y} = y^2(x_2 - q_2),$$

$$\begin{aligned} \dot{q}_2 &= q_2(x_2 - q_2) \left( b + \frac{ay}{1 + ay} \right), \\ \dot{r}_2 &= 0, \end{aligned} \quad (4.24)$$

after division by  $r_2$ . We consider the following set

$$U_2 = \left\{ (x_2, y, q_2, r_2) \mid x_2 \in [-\xi^{-1}, \xi^{-1}] \right\}$$

We enter chart  $\kappa_2$  from chart  $\kappa_1$  (corresponding to initial conditions described in Proposition 4.4) within

$$\Gamma_2 : \quad q_2 = \mu^{1/2}, \quad y = \ln^{-1}\varepsilon^{-1/2}(1 + o(1)), \quad x_2 \in [-c, c], \quad (4.25)$$

with  $c > 0$  large. For  $\varepsilon = 0$  we therefore have  $y = 0$  and only dynamics on  $q_2$ :

$$\begin{aligned} \dot{x}_2 &= 0, \\ \dot{q}_2 &= q_2(x_2 - q_2). \end{aligned} \quad (4.26)$$

Initial conditions within  $\Gamma_2$  with  $x_2 \geq 0$  therefore contract towards

$$C_2 = \{U_2 \mid q_2 = x_2, x_2 \geq 0, r_2 = 0\},$$

while initial conditions with  $x_2 < 0$  contract towards the invariant set

$$I_2 = \{U_2 \mid q_2 = 0\},$$

for  $\varepsilon = 0$ . Here  $I_2$ , as a set of critical points of (4.26), undergoes a transcritical bifurcation at  $x_2 = 0$ , going from asymptotically stable for  $x_2 < 0$  to asymptotically unstable for  $x_2 > 0$ . This produces the set  $C_2$ . This set is just  $C_1$  for  $x_2 \geq \mu^{1/2}$  from chart  $K_1$ . It is non-hyperbolic at  $x_2 = 0$ . Using the following blowup:

$$x_2 = \bar{\rho}\bar{x}_2, \quad y = \bar{\rho}^2\bar{y}, \quad q_2 = \bar{\rho}\bar{q}_2, \quad (\bar{\rho}, (\bar{x}_2, \bar{y}, \bar{q}_2)) \in \bar{\mathbb{R}}_+ \times S^2,$$

and the chart  $\bar{q}_2 = 1$  it is possible to study  $C_2$  and  $M_2 = \kappa_{21}(M_1)$ , recall (4.14), near this singularity. This enable us to guide initial conditions  $x_2 = \mathcal{O}(\ln \varepsilon^{-1})$  along  $M_2$  and eventually back into chart  $K_1$ . This establishes the result of Theorem 4.1



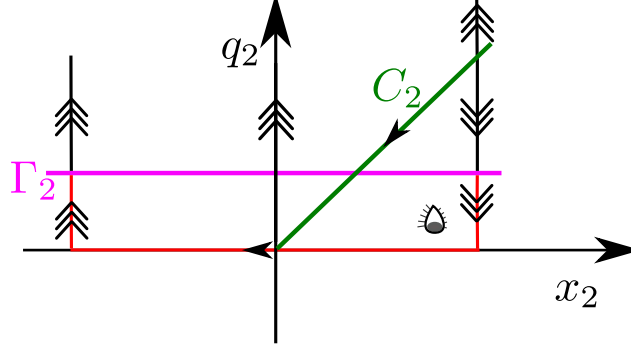


FIGURE 12. Illustration of the delayed stability that causes the transition from canards without head to canards with head. The return mapping to  $\Gamma_2$  is described by Proposition 4.6. We have here used the original orientation of time. Hence, the arrows should be reversed when time is as in (4.23).

for these set of initial conditions. The analysis is very similar to the analysis used in proving Proposition 4.4 so we again skip the details. More interestingly, we note that for  $x_2 < 0$ , we obtain a delayed stability phenomenon due to the attraction (repulsion) of the invariant set  $I_2$  for  $x_2 < 0$  ( $x_2 > 0$ ). In this model, this is where the transition from canards without head to canards with head occurs. See also Fig. 12 where we, for easing the comparison with Fig. 8, use the original direction of time.

We describe the delayed stability in the following proposition:

**Proposition 4.6.** *Consider  $\varepsilon$  sufficiently small and initial conditions in  $\Gamma_2$  with  $x_2 \leq -c^{-1}$ ,  $c > 0$  but large. Then for  $\mu$  sufficiently small the forward flow of (4.23) gives rise to a return mapping  $x_2 \mapsto x_2^+(x_2)$  on  $\Gamma_2$  which satisfies:*

$$x_2^+(x_2) = -x_2 + o(1), \quad (x_2^+)'(x_2) = -1 + o(1),$$

as  $\varepsilon \rightarrow 0$ .

*Proof.* The proof of this statement follows the proof of the delayed stability phenomenon in planar slow-fast systems studied in [33]. This classical result basically uses appropriate lower and upper solutions to properly bound the motion of the fast variable. To translate this into the current context we need to bound  $y$ . For this we note the following: For  $q_2 = 0$  we can write (4.23) as

$$y'(x_2) = \frac{yx_2}{1 + x_2^2 + \alpha y}.$$

The solution through  $y(0) = y_0$  is

$$y = y_0 \frac{\sqrt{(\alpha y_0 + 1)^2 + x_2^2(2\alpha + 1)} + \alpha y_0}{1 + 2\alpha y_0} = y_0 \sqrt{x_2^2 + 1} (1 + \mathcal{O}(y_0)).$$



Therefore for  $\alpha$  sufficiently small we have that  $y$  of (4.9), with initial conditions from (4.25), is bounded as

$$y_0 \sqrt{x_2^2 + 1} (1 - \alpha) \leq y \leq y_0 \sqrt{x_2^2 + 1} (1 + \alpha).$$

Here  $y_0 = \mathcal{O}(\ln^{-1} \varepsilon^{-1})$  cf. the initial conditions (4.25) and  $y_0$  will play the role of the small parameter. From here we can bound the fast variable by considering the following two upper  $\bar{q}_2$  and lower solutions  $\underline{q}_2$  obtained from the following equations:

$$\begin{aligned} \bar{q}_2'(x_2) &= \frac{\bar{q}_2(x_2 + \alpha)}{y_0 \sqrt{x_2^2 + 1} (1 - \alpha)}, \\ \underline{q}_2'(x_2) &= \frac{\underline{q}_2(x_2 - \alpha)}{y_0 \sqrt{x_2^2 + 1} (1 + \alpha)}, \end{aligned}$$

after possibly decreasing  $\alpha$  further. Proceeding as in [33] gives the desired result.  $\square$

From  $x_2^+(x_2)$  we use the attraction of  $C_2$  to follow the trajectory back into chart  $K_1$ . This proves the statement for this set of initial conditions.

**4.6. Final remarks.** The initial conditions within  $X_3$  in (4.22) in chart  $\kappa_1$  can be followed into chart  $\bar{x} = -1$  of (4.12) and then subsequently into charts  $\kappa_2$  and  $\bar{x} = 1$ . These orbits will for decreasing values of  $x_1$  remain closer to  $I_2$  for a longer period of time before jumping towards  $M_2$ . Eventually the fast jump along the critical fibers will occur so that the forward orbit no longer intersects  $\Lambda$  close to  $S_\varepsilon \cap \Lambda$ . In fact, ultimately the forward orbit does not intersect  $S_\varepsilon$  at all. We skip the details of this because this can be obtained without the introduction of  $q$ . For the original model, which is just obtained by reversing time, this gives rise to the transition from canards with head to relaxation oscillations that (a) follow the attracting branch  $\hat{S}_\varepsilon$ , then (b) jump near the fold  $F$  towards infinity. Here (c) the orbit follows  $I_2$  until it (d) takes off along a critical fiber in chart  $K_1$  to return to  $\hat{S}_\varepsilon$ . See Fig. 10. Using the charts  $\bar{x} = \pm 1$  it is straightforward to show that for these orbits the value of  $y$  is  $\mathcal{O}(\sqrt{\varepsilon})$  with respect to  $\varepsilon$  during the passage near  $I_2$ . Using (4.6), we obtain  $u = \mathcal{O}(1/\sqrt{\varepsilon})$  in terms of the original fast variable.

## 5. CONCLUSION

We have presented a novel approach to deal with flat slow manifolds that appear in slow-fast systems. The basic idea of this method is to embed the system into a higher dimensional system for which the standard blowup approach, in the formulation of Krupa and Szmolyan, can be applied to deal with the loss of hyperbolicity. In this paper, we did not aim to put our approach into a general framework (this should be part of future work) but instead we demonstrated its use on two examples: Regularization of PWS systems using tanh and a model of aircraft ground dynamics. In the future, it would also be interesting to pursue applications of our approach to areas outside the realm of the classical geometric singular perturbation theory.



## ACKNOWLEDGEMENT

The author would like to thank C. Kuehn for pointing me in the direction [31], Elena Bossolini, Morten Brøns and Peter Szmolyan for useful discussions, and finally Stephen Schecter for providing valuable feedback.

## APPENDIX A. PROOF OF THEOREM 3.3 USING BLOWUP

We consider the following system

$$\begin{aligned}\dot{x} &= \varepsilon(1 + \phi(\hat{y})), \\ \dot{\hat{y}} &= 2x(1 + \phi(\hat{y})) + 1 - \phi(\hat{y}),\end{aligned}\tag{A.1}$$

with  $\phi \in C_{ST}^{n-1}$ ,  $n \geq 2$  (see Definition 3.1). Here

$$S_a : \phi(\hat{y}) = \frac{1 + 2x}{1 - 2x}, \quad x < 0,$$

is an attracting critical manifold. It loses hyperbolicity at  $(x, \hat{y}) = 0$  in a fold (degenerate for  $n \geq 2$ ; in particular a cusp for  $n = 3$ ). Indeed, the linearization of (A.1) about  $S_a$  gives an eigenvalue

$$(2x - 1)\phi'(\hat{y}).$$

This eigenvalue vanishes at  $\hat{y} = 0$  since  $\phi'(\hat{y}) = 0$  by 3° in Definition 3.1. For  $x \in [c, -\rho]$ ,  $\rho$  sufficiently small, the critical manifold  $S_a$  perturbs to a Fenichel slow manifold  $S_{a,\varepsilon}$ . We will initially seek to guide  $S_{a,\varepsilon}$  up until  $\hat{y} = 1$ . For this we will use the following expansion of  $\phi(\hat{y})$  about  $\hat{y} = 1$

$$\phi(\hat{y}) = 1 - \phi^{[n]}(-\tilde{y})^n(1 + \tilde{y}R(\tilde{y})),$$

and

$$\hat{y} = 1 + \tilde{y}, \quad \phi^{[n]} = \frac{(-1)^{n+1}}{n!} \phi^{(n)}(1) > 0.$$

Here  $R(\tilde{y})$  is smooth by Taylor's theorem. This expression is valid for  $\tilde{y} \in (-2, 0]$  and follows directly from Definition 3.1. This gives the following equations:

$$\begin{aligned}\dot{x} &= \varepsilon, \\ \dot{\tilde{y}} &= 2x + \frac{1}{2} \phi^{[n]}(-\tilde{y})^n(1 + \tilde{y}Q(\tilde{y})).\end{aligned}\tag{A.2}$$

for some smooth  $Q(\tilde{y})$ , after division of the right hand side by

$$1 + \phi(\hat{y}) = 2 - \phi^{[n]}(-\tilde{y})^n(1 + \tilde{y}R(\tilde{y})) > 0 \quad \text{within} \quad \tilde{y} \in (-2, 0).$$

Now we apply the following blowup:

$$x = r^n \bar{x}, \quad \tilde{y} = r \bar{y}, \quad \varepsilon = r^{2n-1} \bar{\varepsilon}, \quad (r, (\bar{x}, \bar{y}, \bar{\varepsilon})) \in \overline{\mathbb{R}}_+ \times S^2,$$

and consider the following two charts:

$$\begin{aligned}\kappa_1 : \quad \bar{y} = -1 : \quad x &= r_1^n x_1, \quad \tilde{y} = -r_1, \quad \varepsilon = r_1^{2n-1} \varepsilon_1, \\ \kappa_2 : \quad \bar{\varepsilon} = 1 : \quad x &= r_2^n x_2, \quad \tilde{y} = r_2 y_2, \quad \varepsilon = r_2^{2n-1}.\end{aligned}$$



A.1. **Chart  $\kappa_1$ .** In this chart we obtain the following system:

$$\begin{aligned}\dot{x}_1 &= \epsilon_1 + x_1 \left( 2x_1 + \frac{1}{2}\phi^{[n]}(1 - r_1 Q(-r_1)) \right), \\ \dot{r}_1 &= -r_1 \left( 2x_1 + \frac{1}{2}\phi^{[n]}(1 - r_1 Q(-r_1)) \right), \\ \dot{\epsilon}_1 &= (2n-1) \left( 2x_1 + \frac{1}{2}\phi^{[n]}(1 - r_1 Q(-r_1)) \right) \epsilon_1,\end{aligned}$$

after desingularization through the division by  $r_1^{n-1}$  on the right hand side. In this chart  $S_a$  becomes

$$S_{a,1}: \quad x_1 = -\frac{1}{4}\phi^{[n]}(1 - r_1 Q(-r_1)), \quad r_1 \geq 0.$$

We consider the following set

$$U_1 = \{(x_1, r_1, \epsilon_1) | x_1 \in [-\xi^{-1}, 0], r_1 \in [0, \rho], \epsilon_1 = [0, \nu]\},$$

with  $\xi, \rho, \nu$  sufficiently small. Center manifold theory applied to the equilibrium  $x_1 = -\frac{1}{4}\phi^{[n]}, r_1 = \epsilon_1 = 0$  as a partially hyperbolic equilibrium gives the following:

**Proposition A.1.** *There exists a center manifold within  $U_1$ :*

$$M_1: \quad x_1 = -\frac{1}{4}\phi^{[n]}(1 - r_1 Q(-r_1)) + \epsilon_1 m_1(r_1, \epsilon_1),$$

with

$$m_1(r_1, \epsilon_1) = \frac{2}{\phi^{[n]}} + \mathcal{O}(r_1 + \epsilon_1).$$

The manifold  $M_1$  is foliated by invariant hyperbolas

$$E_1: \quad \epsilon = r_1^{2n-1} \epsilon_1,$$

and contains the critical manifold  $S_{a,1}$  within  $\epsilon_1 = 0$ , as a set of critical points, and

$$C_{a,1}: \quad x_1 = -\frac{1}{4}\phi^{[n]} + \epsilon_1 m_1(0, \epsilon_1),$$

within  $r_1 = 0$ , as a unique center sub-manifold.

*Proof.* The proof of this is straightforward. The uniqueness of  $C_{a,1}$  follows from the fact that  $\dot{\epsilon}_1 > 0$  within  $C_{a,1} \cap \{\epsilon_1 > 0\}$ .  $\square$

**Remark A.2.** As usual  $M_1 \cap E_1$  is  $\mathcal{O}(e^{-c/\epsilon})$ -close to Fenichel's slow manifold  $S_{a,\epsilon,1}$  at  $r_1 = \rho$  and we shall therefore view  $M_1 \cap E_1$  as the extension of Fenichel's slow manifold. At  $\epsilon_1 = \nu$  we have  $r_1 = (\nu^{-1}\epsilon)^{1/(2n-1)}$  within  $E_1$  and therefore the proposition provides an extension of  $S_{a,\epsilon,1}$  satisfying:

$$S_{a,\epsilon,1} \cap \{\epsilon_1 = \nu\}: \quad x_1 = -\frac{1}{4}\phi^{[n]} + \nu m_1(0, \nu) + \epsilon^{1/(2n-1)} Q_1(\epsilon^{1/(2n-1)}), \quad (\text{A.3})$$

with  $Q_1$  smooth. In other words,  $S_{a,\epsilon,1}$  is  $\epsilon^{1/(2n-1)}$ -smoothly close to  $C_{a,1}$  at  $\epsilon_1 = \nu$ .

We continue  $S_{a,\epsilon,1}$  into chart  $\kappa_2$  in the following. For this we will use the closeness of  $S_{a,\epsilon,1}$  to  $C_{a,1}$  and therefore guide  $S_{a,\epsilon,1}$  by following  $C_{a,1}$ . The change of coordinates between  $\kappa_1$  and  $\kappa_2$  is given as

$$x_2 = \epsilon_1^{-n/(2n-1)} x_1, \quad y_2 = -\epsilon_1^{-1/(2n-1)}, \quad r_2 = r_1 \epsilon_1^{1/(2n-1)}.$$

We will denote  $C_{a,1}$  and  $S_{a,\epsilon,1}$  by  $C_{a,2}$  and  $S_{a,\epsilon,2}$ , respectively, in chart  $\kappa_2$ .



A.2. **Chart  $\kappa_2$ .** Insertion gives

$$\begin{aligned}\dot{x}_2 &= 1, \\ \dot{y}_2 &= 2x_2 + \frac{1}{2}\phi^{[n]}(-y_2)^n(1 + r_2 y_2 Q(r_2 y_2)), \\ \dot{r}_2 &= 0,\end{aligned}\tag{A.4}$$

after desingularization through division of the right hand side by  $r_2^{n-1}$ . We have

**Lemma A.3.** *The forward flow of  $C_{a,2} \subset \{r_2 = 0\}$  intersects  $y_2 = 0$  in*

$$(x_2, y_2, r_2) = (c_x \eta(n), 0, 0),$$

where  $\eta(n)$  only depends upon  $n$  and

$$c_x = \left( \frac{2}{\phi^{[n]}} \right)^{1/(2n-1)}.\tag{A.5}$$

*Proof.* We scale  $x_2$  and  $y_2$  by introducing:

$$x_2 = c_x u, \quad y_2 = c_y v,$$

with  $c_x$  as in (A.5) and

$$c_y = -2c_x^2.$$

This transforms (A.4) into

$$\begin{aligned}\dot{u} &= 1, \\ \dot{v} &= -u - v^n,\end{aligned}$$

for  $r_2 = 0$  and  $v \geq 0$ , after scaling time by  $c_x$ . The result then follows from [32, Proposition 3.10].  $\square$

Now, using the  $\varepsilon^{1/(2n-1)}$ -smooth closeness of  $S_{a,\varepsilon,2}$  to  $C_{a,2}$  at  $y_2 = -\nu^{-1/(2n-1)}$ , we can apply regular perturbation theory and blow back down to conclude the following:

**Proposition A.4.** *The forward flow of Fenichel's slow manifold  $S_{a,\varepsilon}$  intersects  $\hat{y} = 1$  in  $(x, \hat{y}) = (x_\varepsilon, 1)$  with*

$$x_\varepsilon = r_2^n \left( \frac{2}{\phi^{[n]}} \right)^{1/(2n-1)} \eta(n) (1 + r_2 Q_2(r_2)),\tag{A.6}$$

with  $Q_2(r_2)$  smooth.

A.3. **Scaling down.** To continue  $S_{a,\varepsilon}$  beyond  $\hat{y} = 1$  and towards  $x = \delta$  we scale back down using (3.8) and return to the  $(x, y)$ -variables:

$$\begin{aligned}\dot{x} &= 1, \\ \dot{y} &= 2x.\end{aligned}$$

We then use  $(x, y) = (x_\varepsilon, \varepsilon)$  as an initial condition and obtain, through simple integration,

$$y_\theta(\varepsilon) = \theta^2 + \varepsilon - x_\varepsilon^2,$$

at  $x = \theta$ . This then completes the proof of Theorem 3.3.



## APPENDIX B. PROOF OF THEOREM 3.4 BY DIRECTION INTEGRATION

The system (3.9) with  $\phi(\hat{y}) = \tanh(\hat{y})$  can be written as

$$\frac{dy}{dx} = 2x + \frac{1 - \tanh(y\epsilon^{-1})}{1 + \tanh(y\epsilon^{-1})} = 2x + e^{-2y\epsilon^{-1}},$$

upon elimination of time and returning to  $y$  through (3.8). Integrating this gives

$$y(x) = x^2 + \frac{1}{2}\epsilon \ln \left( \sqrt{\frac{\pi}{2\epsilon}} \left( \operatorname{erf} \left( \sqrt{2\epsilon^{-1}}x \right) + C \right) \right),$$

where  $C$  is an integration constant and

$$\operatorname{erf}(u) = \frac{2}{\sqrt{\pi}} \int_0^u e^{-s^2} ds,$$

is the Gauss error function satisfying

$$\operatorname{erf}(u) = \pm 1 - \frac{e^{-u^2}}{\sqrt{\pi}u} (1 + \mathcal{O}(u^{-2})) \quad \text{for } u \rightarrow \pm\infty \quad (\text{B.1})_{\pm}$$

By (B.1)<sub>-</sub> it follows that the solution with  $C = 1$ :

$$y(x) = x^2 + \frac{1}{2}\epsilon \ln \left( \sqrt{\frac{\pi}{2\epsilon}} \left( \operatorname{erf} \left( \sqrt{2\epsilon^{-1}}x \right) + 1 \right) \right),$$

does not contain any fast components. It therefore represents a geometrically unique slow manifold. Now using (B.1)<sub>+</sub> we obtain

$$y(\theta) = \theta^2 + \epsilon \left( \frac{1}{4} \ln(2\pi\epsilon^{-1}) + \mathcal{O}(e^{-2\epsilon^{-1}\theta^2}) \right),$$

in agreement Theorem 3.4.

## REFERENCES

- [1] E. Bossolini, M. Brøns, and K. Uldall Kristiansen. Singular limit analysis of the BKR model for Earthquake Faulting. *In preparation*, 2016.
- [2] M. Brøns. Canard explosion of limit cycles in templator models of self-replication mechanisms. *Journal of Chemical Physics*, 134(144105), 2011.
- [3] M. di Bernardo, C. J. Budd, A. R. Champneys, and P. Kowalczyk. *Piecewise-smooth Dynamical Systems: Theory and Applications*. Springer Verlag, 2008.
- [4] F. Dumortier. Local study of planar vector fields: Singularities and their unfoldings. In H. W. Broer et al, editor, *Structures in Dynamics, Finite Dimensional Deterministic Studies*, volume 2, pages 161–241. Springer Netherlands, 1991.
- [5] F. Dumortier. Techniques in the theory of local bifurcations: Blow-up, normal forms, nilpotent bifurcations, singular perturbations. In Dana Schlomiuk, editor, *Bifurcations and Periodic Orbits of Vector Fields*, volume 408 of *NATO ASI Series*, pages 19–73. Springer Netherlands, 1993.
- [6] F. Dumortier and R. Roussarie. Canard cycles and center manifolds. *Mem. Amer. Math. Soc.*, 121:1–96, 1996.
- [7] B. Erickson, B. Birnir, and D. Lavalle. A model for aperiodicity in earthquakes. 2008.
- [8] N. Fenichel. Persistence and smoothness of invariant manifolds for flows. *Indiana University Mathematics Journal*, 21:193–226, 1971.
- [9] N. Fenichel. Asymptotic stability with rate conditions. *Indiana University Mathematics Journal*, 23:1109–1137, 1974.
- [10] V. Gelfreich and L. Lerman. Almost invariant elliptic manifold in a singularly perturbed Hamiltonian system. *Nonlinearity*, 15:447–557, 2002.
- [11] Michael G. Hayes, Tasso J. Kaper, Peter Szmolyan, and Martin Wechselberger. Geometric desingularization of degenerate singularities in the presence of fast rotation: A new proof of known results for slow passage through Hopf bifurcations. *Indagationes Mathematicae*, 2015.



- [12] E. M. Izhikevich. *Dynamical Systems in Neuroscience: The geometry of Excitability and Bursting*. The MIT Press, 2007.
- [13] C.K.R.T. Jones. *Geometric Singular Perturbation Theory, Lecture Notes in Mathematics, Dynamical Systems (Montecatini Terme)*. Springer, Berlin, 1995.
- [14] T. Kaper. An introduction to geometric methods and dynamical systems theory for singular perturbation problems. *Proceedings of Symposia in Applied Mathematics*, 56, 1999.
- [15] I. Kosiuk and P. Szmolyan. Geometric singular perturbation analysis of an autocatalator model. *Discrete and Continuous Dynamical Systems - Series S*, 2(4):783–806, 2009.
- [16] I. Kosiuk and P. Szmolyan. Scaling in singular perturbation problems: Blowing up a relaxation oscillator. *Siam Journal on Applied Dynamical Systems*, *Siam J. Appl. Dyn. Syst.*, *Siam J a Dy*, *Siam J Appl Dyn Syst*, *Siam Stud Appl Math*, 10(4):1307–1343, 2011.
- [17] I. Kosiuk and P. Szmolyan. Geometric analysis of the Goldbeter minimal model for the embryonic cell cycle. *Journal of Mathematical Biology*, *J. Math. Biol.*, *J Math Biol*, 2015.
- [18] K. U. Kristiansen. Periodic orbits near a bifurcating slow manifold. *Journal of Differential Equations*, 259(9):4561–4614, 2015.
- [19] K. U. Kristiansen and C. Wulff. Exponential estimates of symplectic slow manifolds. *ArXiv e-prints*, August 2012.
- [20] K. Uldall Kristiansen and S. J. Hogan. On the use of blowup to study regularizations of singularities of piecewise smooth dynamical systems in  $\mathbb{R}^3$ . *SIAM Journal on Applied Dynamical Systems*, 14(1):382–422, 2015.
- [21] K. Uldall Kristiansen and S. J. Hogan. Regularizations of two-fold bifurcations in planar piecewise smooth systems using blowup. *SIAM Journal on Applied Dynamical Systems*, 14(4):1731–1786, 2015.
- [22] K. Uldall Kristiansen and S. J. Hogan. On the interpretation of the piecewise smooth visible-invisible two-fold singularity in  $\mathbb{R}^3$  using regularization and blowup. *arXiv:1602.01026*, 2016.
- [23] M. Krupa and P. Szmolyan. Extending geometric singular perturbation theory to nonhyperbolic points - fold and canard points in two dimensions. *SIAM Journal on Mathematical Analysis*, 33(2):286–314, 2001.
- [24] M. Krupa and P. Szmolyan. Extending slow manifolds near transcritical and pitchfork singularities. *Nonlinearity*, 14(6):1473, 2001.
- [25] M. Krupa and P. Szmolyan. Relaxation oscillation and canard explosion. *Journal of Differential Equations*, 174(2):312–368, 2001.
- [26] C. Kuehn. Normal hyperbolicity and unbounded critical manifolds. *Nonlinearity*, 27(6):1351, 2014.
- [27] C. Kuehn. *Multiple Time Scale Dynamics*. Springer-Verlag, Berlin, 2015.
- [28] J. Llibre, P. R. da Silva, and M. A. Teixeira. Sliding vector fields via slow-fast systems. *Bulletin of the Belgian Mathematical Society-Simon Stevin*, 15(5):851–869, 2008.
- [29] A. I. Neishtadt. Persistence of stability loss for dynamical bifurcations .1. *Differential Equations*, 23(12):1385–1391, 1987.
- [30] A. I. Neishtadt. Persistence of stability loss for dynamical bifurcations .2. *Differential Equations*, 24(2):171–176, 1988.
- [31] J. Rankin, M. Desroches, B. Krauskopf, and M. Lowenberg. Canard cycles in aircraft ground dynamics. *Nonlinear Dynamics*, 66(4):681–688, 2011.
- [32] C. B. Reves and T. M. Seara. Regularization of sliding global bifurcations derived from the local fold singularity of Filippov systems. *arXiv preprint arXiv:1402.5237*, 2014.
- [33] S. Schecter. Persistent unstable equilibria and closed orbits of a singularly perturbed equations. *Journal of Differential Equations*, 60:131–141, 1985.
- [34] J. Sotomayor and M. A. Teixeira. Regularization of discontinuous vector fields. In *Proceedings of the International Conference on Differential Equations, Lisboa*, pages 207–223, 1996.
- [35] V. I. Utkin. Variable structure systems with sliding modes. *IEEE Trans. Automatic Control*, 22:212–222, 1977.